Accepted Manuscript

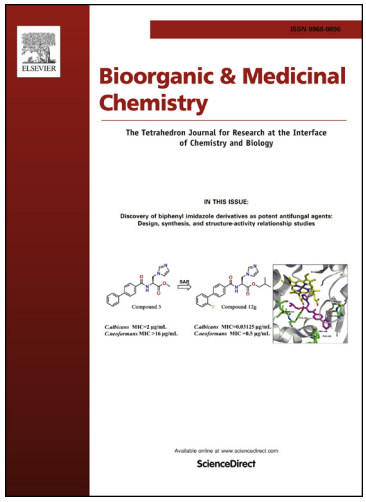

Design and synthesis of selective CDK8/19 dual inhibitors: Discovery of 4,5-dihydrothieno[3',4':3,4]benzo[1,2-*d*]isothiazole derivatives

Koji Ono, Hiroshi Banno, Masanori Okaniwa, Takaharu Hirayama, Naoki Iwamura, Yukiko Hikichi, Saomi Murai, Maki Hasegawa, Yuka Hasegawa, Kazuko Yonemori, Akito Hata, Kazunobu Aoyama, Douglas R. Cary

PII: S0968-0896(16)31440-7
DOI: http://dx.doi.org/10.1016/j.bmc.2017.02.038
Reference: BMC 13568

To appear in: *Bioorganic & Medicinal Chemistry*

Received Date: 21 December 2016
Revised Date: 17 February 2017
Accepted Date: 17 February 2017

Please cite this article as: Ono, K., Banno, H., Okaniwa, M., Hirayama, T., Iwamura, N., Hikichi, Y., Murai, S., Hasegawa, M., Hasegawa, Y., Yonemori, K., Hata, A., Aoyama, K., Cary, D.R., Design and synthesis of selective CDK8/19 dual inhibitors: Discovery of 4,5-dihydrothieno[3',4':3,4]benzo[1,2-*d*]isothiazole derivatives, *Bioorganic & Medicinal Chemistry* (2017), doi: http://dx.doi.org/10.1016/j.bmc.2017.02.038

Design and synthesis of selective CDK8/19 dual inhibitors: Discovery of 4,5-dihydrothieno[3',4':3,4]benzo[1,2-*d*]isothiazole derivatives

Koji Ono,[a, *] Hiroshi Banno,[a] Masanori Okaniwa,[a] Takaharu Hirayama,[a] Naoki Iwamura,[b] Yukiko Hikichi,[c] Saomi Murai,[a] Maki Hasegawa,[a] Yuka Hasegawa,[a] Kazuko Yonemori,[a] Akito Hata,[a] Kazunobu Aoyama,[a] and Douglas R. Cary[a, †]

[a] *Pharmaceutical Research Division, Takeda Pharmaceutical Co., Ltd., Shonan Research Center, 26-1, Muraoka-Higashi 2-Chome, Fujisawa, Kanagawa 251-8555, Japan*

[b] *Takeda Union, 26-1, Muraoka-Higashi 2-Chome, Fujisawa, Kanagawa 251-8555, Japan*

[c] *Product Information Group Japan Oncology Business Unit, Takeda Pharmaceutical Co., Ltd., 12-10, Nihonbashi 2-Chome, Chuo-ku, Tokyo 103-8686, Japan*

* Corresponding author. Tel.: +81 466 32 1168; fax: +81 466 29 4448.

E-mail address: kouji.ono@takeda.com (K. Ono)

[†] Present address: *Peptidream Inc.*

Abstract

To develop a novel series of CDK8/19 dual inhibitors, we employed structure-based drug design using docking models based on a library compound, 4,5-dihydroimidazolo[3',4':3,4]benzo[1,2-*d*]isothiazole **16** bound to CDK8. We designed various [5,6,5]-fused tricyclic scaffolds bearing a carboxamide group to maintain predicted interactions with the backbone C=O and NH of Ala100 in the CDK8 kinase hinge region. We found that 4,5-dihydrothieno[3',4':3,4]benzo[1,2-*d*]isothiazole derivative **29a** showed particularly potent enzymatic inhibitory activity in both CDK8/19 (CDK8 IC_{50}: 0.76 nM, CDK19 IC_{50}: 1.7 nM). To improve the physicochemical properties and kinase selectivity of this compound, we introduced a substituted 3-pyridyloxy group into the scaffold 8-position. The resulting optimized compound **52h** showed excellent in vitro potency (CDK8 IC_{50}: 0.46 nM, CDK19 IC_{50}: 0.99 nM), physicochemical properties, and kinase selectivity (only 5 kinases showed <35% unbound fraction at 300 nM. CDK19: 4.6%, CDK8: 8.3%, HASPIN: 23%, DYRK1B: 27%, HIP1: 32%). Based on a docking model of **52h** bound to CDK8, we could explain the highly specific kinase activity profile found for this compound, based on the interaction of the pyridyl group of **52h** interacting with Met174 of the CDK8 DMG activation loop.

In vitro pharmacological evaluation of **52h** revealed potent suppression of phosphorylated STAT1 in various cancer cells. The high oral bioavailability found for this compound enabled in vivo studies, in which we demonstrated a mechanism-based in vivo PD effect as well as tumor growth suppression in an RPMI8226 human hematopoietic and lymphoid xenograft model in mouse [T/C: −1% (2.5 mg/kg, qd)].

Graphical abstract

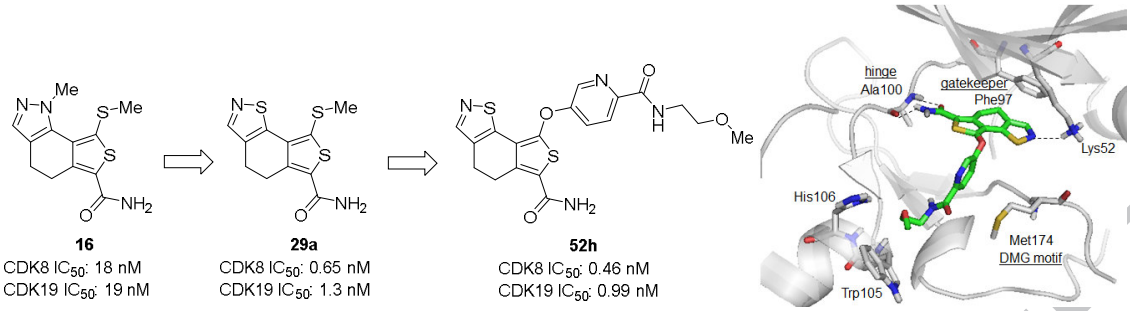

Keywords

CDK8; CDK19; Cyclin-dependent kinases (CDKs); transcriptional regulation; STAT1; RPMI8226; SW480; DMG; 4,5-dihydrothieno[3',4':3,4]benzo[1,2-*d*]isothiazole

1. Introduction

Cyclin-dependent kinases (CDKs)[1] are serine/threonine kinases that are regulated through their interaction with a cyclin subunit. CDKs are categorized based on their action through one of two different biological mechanisms: CDKs that play an important role in cell cycle regulation by binding to multiple cyclins, and CDKs that control transcriptional regulation by binding to a single cyclin. In mammals, the CDK family is grouped into the cell cycle-related (CDK1, CDK2, CDK4/6, etc.) and transcriptional (CDK7, CDK8, CDK9, CDK12, CDK19, etc.) subfamilies. Although various pan-CDK inhibitors known to function as cell-cycle regulators have demonstrated antitumor efficacy in clinical trials,[2] the antitumor activity of some of these have been reported as also arising from their effects on transcriptional regulation through the inhibition of CDK7 and CDK9, which are members of the transcriptional CDK subfamily.[3]

CDK8 has been reported to act as a transcriptional regulator,[4] and has been found to be overexpressed in colorectal cancer (CRC) and adenocarcinoma relative to adjacent normal tissue.[5] Furthermore, CDK8 was identified as a major oncogenic driver for amplification at 13q12.13–12q12.2 in CRC in two RNA interference-based loss-of-function screens.[6] Immunohistochemical analysis of the CDK8 expression correlated with the tumor grade, stage and the local recurrence or metastasis in extrauterine leiomyosarcoma,[7] and is associated with shorter relapse-free survival in breast cancer.[8]

CDK8 plays various roles in different signaling pathways to modulate gene expression levels as a part of the Mediator complex (CDK8, MED12, MED13, and cyclin-C),[9] such as in the regulation of RNA polymerase (RNAP) II,[10] activation at the nucleosome level by phosphorylation at Ser10 of histone H3,[11] enhancement of β-catenin dependent gene expression by phosphorylation of E2F1,[6a, 10c, 10f, 12] activation of INFγ-dependent gene expression by phosphorylation of STAT1,[13] inhibition of Notch1-dependent gene expression by phosphorylation of ICN1,[14] modulation of TGF-β signaling,[10c, 15] and regulation of p27 protein expression by Skp2-mediated p27 ubiquitination and degradation.[16]

These biological effects of CDK8 on context-related gene expression may be beneficial for patients suffering from various types of tumors. [4, 17] Current pan-CDK inhibitors in clinical trials have potential risks, such as narrow therapeutic windows due to their indiscriminate toxicity toward normal cells,

and complications in attempting to understand their mechanisms of action.[1, 2] Therefore, a highly selective inhibitor of CDK8 could be a promising candidate for cancer therapy. Although CDK19[10c, 12b, 18] is closely related to CDK8 in terms of structure and its association with C-type cyclins, its biological role is unclear.

Several classes of small molecules that modulate CDK8 activity have been reported in the patent literature (Figure 1). A quinazoline derivative, Senexin B (SNX2-1–165, **1**),[19] showed CDK8 enzyme inhibitory activity with an IC_{50} value of 24–50 nM in different assay[19b], and displayed potent, selective enzymatic inhibitory activity against CDK8 and CDK19 compared with other CDK family kinases. Furthermore, Senexin B inhibited β-catenin activity in human colon HCT-116 cancer cells, and demonstrated suppression of tumor growth in various types of in vivo model. Macrocyclic compound **2**[20] showed CDK8 binding activity with an IC_{50} value of 31 nM in LanthaScreen™ assay, and also regulated transcriptional activity of β-catenin with an EC_{50} value of 337 nM in reporter assay with human colon HCT-116 cancer cells. Benzimidazole **3**[21] inhibited CDK8 enzyme activity by 96% at 1 μM in an ADP-GLo™ assay, and demonstrated good kinase selectivity against the CDK family (CDK1, 2, 5, 7, 9). Furthermore, **3** showed cell growth inhibitory activity against various cancer cell lines, and demonstrated tumor growth inhibition in NOD/SCID mice bearing a HCT116 tumor xenograft. Pyrazine **4**[22] and pyridine **5**[23], based on similar scaffolds, demonstrated enzyme inhibitory activity against CDK8 bound to cyclin C with IC_{50} values of 0.4 nM and 0.2 nM, respectively, in a LANCE® TR-FRET assay. Pyrrole **6**[24] showed CDK8 enzyme inhibitory activity with an IC_{50} value of 7.0 nM in a LANCE® TR-FRET assay, and displayed anti-proliferative activity against human gastric AGS and colorectal HCT116 cancer cells in vitro. Tricyclic compound **7**[25] showed enzyme inhibitory activity for CDK8 with an IC_{50} value of 22 nM against human lung carcinoma A549 live cells in a mass spectrometry assay using the KiNativ™ platform.

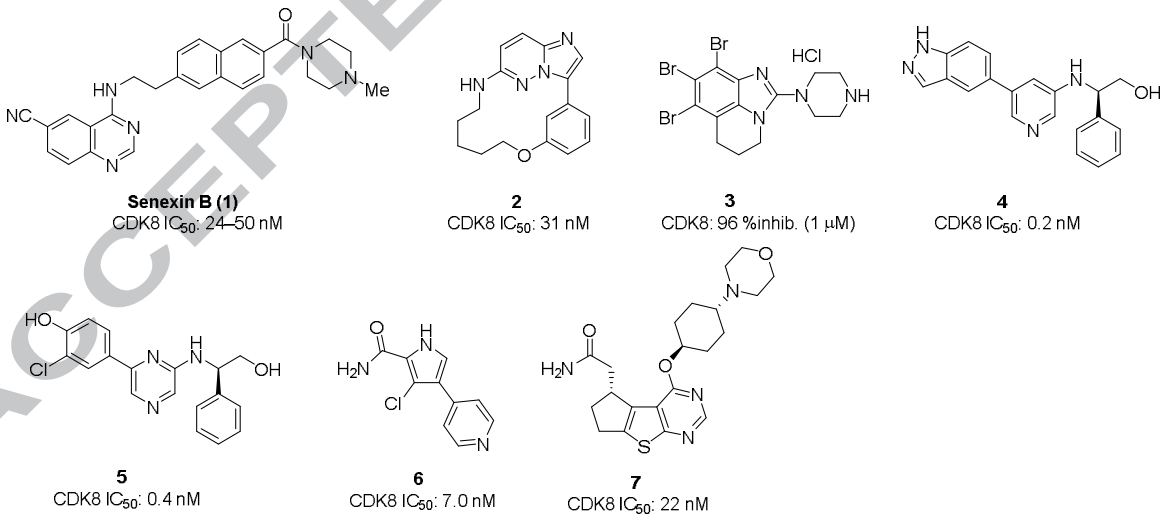

Figure 1. Chemical structures of reported CDK8 inhibitors from the patent literature.

Recently, new mechanistic insights into the potential of CDK8 and CDK19 inhibition in cancer therapy were revealed by the discovery of high-quality small molecule probes (Type I kinase inhibitors shown in Figure 2).[26] The natural product Cortistatin A (**8**)[27] selectively inhibited the kinase activity of the

CDK8/CDK19 module in phosphorylation of the RNAP II C-terminal domain (CTD) with a CDK8 IC_{50} value of 12 nM in vitro, and also showed the complete selectivity against 387 kinases in cell lysate using KiNativ.™ Furthermore, Cortistatin A afforded efficacy in a disseminated human AML model, and 71% tumor volume reduction in an AML xenograft model using SET-2 cells by intraperitoneal injection. The antiproliferative and cell lineage-specific activity of Cortistatin A was caused by the enhancement of master cell fate-determining tumor-suppressor genes regulated by superenhancers.[26a] Identification of Mediator kinase substrates targeted by CDK8 and CDK19 using Cortistatin A suggested effects on pathways implicated in inflammation, growth, and metabolic regulation.[28] In another report, an orally bioavailable small molecule CCT251545 (**9**)[29], which was discovered through cell-based WNT pathway screening, was found to be a CDK8 and CDK19 selective inhibitor with an IC_{50} value of 7.2 nM against CDK8 in Lanthascreen TR-FRET assay.[30] This compound was also found to show >100-fold selectivity against 291 kinases in vitro.[26b] Further optimization to improve metabolic stability lead to the identification of CCT251921 (**10**)[29a, 30] as a good compromise between in vitro biochemical and pharmacokinetic properties. CCT251921 showed strong affinity for CDK8 with an IC_{50} value of 2.3 nM in Lanthascreen TR-FRET assay, and demonstrated potent inhibition of reporter-based readouts measuring basal WNT pathway activity in human cancer cell lines LS174T (β-catenin mutant), SW480, Colo205 (APC mutant), and PA-1 (human teratocarcinoma). On the other hand, scaffold hopping from the 3,4,5-trisubstituted pyridine series lead to the identification of 4,6-disubstituted-isoquinoline derivative **11**,[31] which showed strong binding affinity for CDK8 with an IC_{50} value of 5.1 nM in Lanthascreen TR-FRET assay. Furthermore, CCT251921 and compound **11** suppressed tumor growth in vivo in an APC-mutant SW620 human colorectal carcinoma xenograft model.

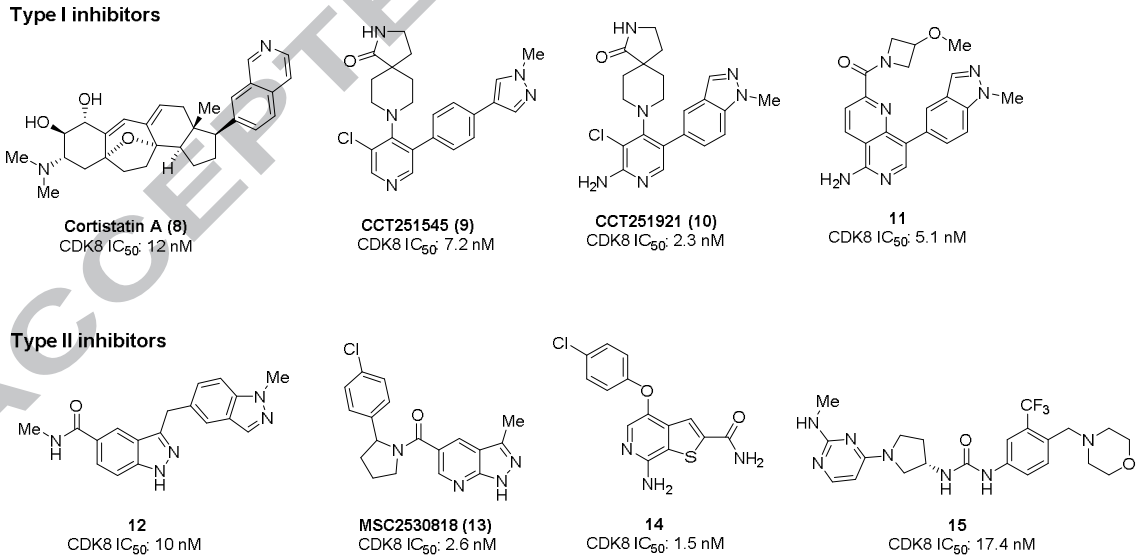

Figure 2. Chemical structures of reported CDK8 inhibitors in the journal literature.

Three additional Type I CDK8 and CDK19 kinase inhibitors have also been recently reported. Orally available 3-benzylindazole **12**[32] was discovered by optimization of compounds with HSP90 affinity to yield potent and selective CDK8 inhibitors. Compound **12** showed strong binding activity for CDK8 with an IC_{50} value of 10 nM in Lanthascreen TR-FRET assay. MSC2530818 (**13**),[33] which was identified by the modification of an imidazothiazole compound, is also an orally available potent and selective CDK8 inhibitor with an IC_{50} value of 2.6 nM in Lanthascreen TR-FRET assay. Both compounds **12** and **13** demonstrated reduction of tumor growth rates in human SW620 colorectal carcinoma xenograft model. Thieno[2,3-c]pyridine compound **14**[34] was also discovered to be a Type I CDK8 and CDK19 inhibitor, with strong affinity for CDK8 indicated by an IC_{50} value of 1.5 nM in Lanthascreen TR-FRET assay. However, CDK8 dependent antiproliferative activity of compound **14** in HCT116 colon cancer cell lines was not observed, despite the confirmation of STAT1 phosphorylation inhibition at Ser727. The modification of the well-known kinase inhibitor Sorafenib also led to the identification of a highly potent and selective Type II CDK8 inhibitor **15**,[35] which showed high binding affinity in Lanthascreen TR-FRET assay (IC_{50}: 17.4 nM). However, compound **15** did not significantly suppress phosphorylation of STAT1 at Ser727.

As stated above, CDK8 inhibition is expected to be a promising approach for treating cancer, however none of the compounds mentioned appear to have entered into clinical studies at this time.

The 4,5-dihydroimidazolo[3',4':3,4]benzo[1,2-*d*]isothiazole derivative **16** (Figure 3), bearing a unique [5,6,5]-fused tricyclic scaffold, was originally identified in our laboratories as a potential prophylactic or therapeutic drug for treating bone or articular diseases, possessing the ability to induce cell differentiation in osteoblasts and chondrocyte precursor cells; later reports focused on the use of these compounds to regulate muscle and fat cell differentiation.[36] However, the target protein of this compound remained unknown for several years. Recently, this compound was screened by affinity selection-mass spectrometry (AS/MS) against a library of approximately 13,000 proteins, and found to bind specifically to CDK19.[37] High throughput screening of an in-house compound library against CDK8 confirmed that a variety of 4,5-dihydroimidazolo[3',4':3,4]benzo[1,2-*d*]isothiazole derivatives, including **16**, inhibit both CDK8 and CDK19 (IC_{50}: 18 nM and 19 nM, respectively). These results prompted us to initiate a campaign to discover novel, potent CDK8/19 dual inhibitors for use in anticancer therapy.

A docking model (shown in Figure 3) was constructed of **16** bound to CDK8 using the program GOLD, version 5.2, and the reported co-crystal structure of CDK8 bound to a small molecule inhibitor (PDB ID: 4F6W).[38] An amide proton and the carbonyl group of the aminocarbonyl moiety at the 4,5-dihydroimidazolo[3',4':3,4]benzo[1,2-d]isothiazole 6-position were suggested to be involved in interaction with the backbone C=O and NH of Ala100 in the kinase hinge region of CDK8. The nitrogen atom at the N-2 position of this scaffold was implicated as being involved in a hydrogen bond with $^{+}NH_3$ of Lys52. Additionally, the methyl sulfide group at the 8-position of this scaffold was directed toward the front pocket region, which consists of a large hydrophobic space. On the basis of these modeling studies, a series of novel CDK8/19 dual inhibitors based on [5,6,5]-fused tricyclic scaffolds were designed (Figure 4). An aryl group introduced into the 8-position of this scaffold was expected to occupy the hydrophobic front

pocket region to improve CDK8 potency and kinase selectivity, while allowing for the modification of ADME properties.

We report herein the synthesis and structure–active relationships (SARs) for a series of tricyclic 4,5-dihydrothieno[3',4':3,4]benzo[1,2-d]isothiazole compounds as novel CDK8/19 dual inhibitors.[39] The optimization of this series led to the identification of **52h**, which showed the antitumor efficacy in a RPMI8226 human hematopoietic and lymphoid xenograft model in mice.

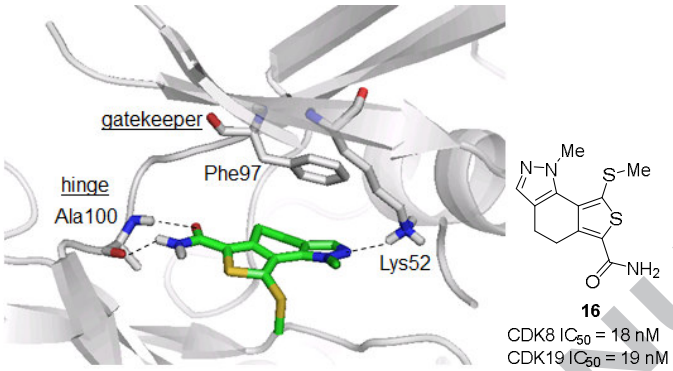

Figure 3. Modeling prediction of compound **16** binding to CDK8 kinase.

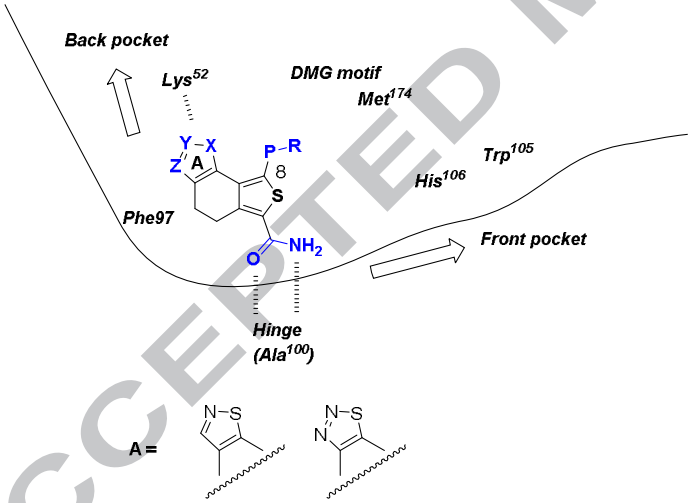

Figure 4. Design of CDK8/19 inhibitors with alternative fused heterocyclic ring A and functionalized at the scaffold 8-position.

2. Chemistry

The 8-methylsulfanyl-4,5-dihydro-1*H*-thieno[3,4-*g*]isothiadizaole scaffold was synthesized from commercially available 1,3-dioxolane-2,1'-cyclohexane-4-one **17** (Scheme 1). The isothiadizaole ring was formed with $SOCl_2$ from *N*-carboxamide hydrazine imine **19**, which was prepared from **17** and

hydrazinecarboxamide **18**. Aldol reaction of **20** with carbon disulfide and the subsequent methylation with MeI afforded the precursor **21** of the desired tricyclic scaffold. Thiophene ring formation was successfully achieved by the treatment of **21** with ethyl 2-mercaptacetate under basic conditions. Transformation of ethyl ester **22** to carboxamide **24** was conducted by hydrolysis with aqueous NaOH, followed by condensation with NH_4Cl and HATU.

Scheme 1. Synthesis of 4,5-dihydro-1*H*-thieno[3,4-*g*]isothiadiazole scaffold.

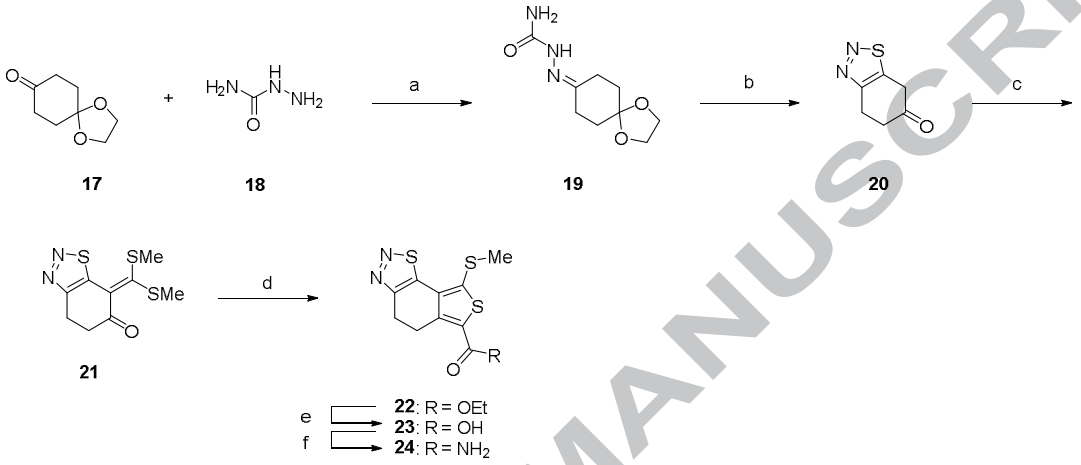

[a]Reagents and conditions: (a) NaOAc, MeOH, rt, 83%; (b) $SOCl_2$, CH_2Cl_2, 0 °C, 10%; (c) CS_2, K_2CO_3, DMF, 0–5 °C, then MeI, 0–5 °C, 23% in 2 steps; (d) $HSCH_2CO_2Et$, K_2CO_3, EtOH, reflux, 50%; (e) NaOH, water/THF/EtOH, rt, 99%; (f) NH_4Cl, HATU, DMF, rt, 86%.

The synthetic procedure for the preparation of the 8-methylsulfanyl-4,5-dihydro-1*H*-thieno[3,4-*g*] isothiazole scaffold is shown in Scheme 2. Vilsmeier–Haack reaction of commercially available **25** with PBr_3 and DMF gave formyl derivative **26** in 39% yields. Isothiazole ring formation of **26** with sodium thiocyanate afforded the desired tricyclic derivative **27**. Transformation of ethyl ester **27** to carboxamide **29a** was conducted by hydrolysis with aqueous NaOH, followed by condensation with aqueous ammonia via acid chloride formation with oxalyl chloride. Dehydration of the carboxyl group of **29a** with $POCl_3$ provided nitrile derivative **30**.

N-Substituted carboxamide derivatives **29b–h** were synthesized by two methods (Scheme 3). The direct condensation of carboxylic acid **28** using HATU in the presence of NMM provided **29b–d**, **f** in 36–76% yields. Stepwise amidation via acid chloride **31**, obtained from **28** by treatment with $SOCl_2$, afforded **29e, g, h** in 13–28% overall yield in two steps.

Scheme 2. Synthesis of 4,5-dihydro-1*H*-thieno[3,4-*g*]isothiazole scaffold.

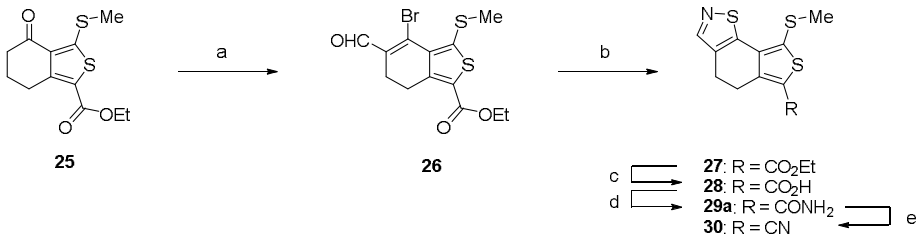

[a]Reagents and conditions: (a) PBr_3, DMF, DME, 80 °C, 39%; (b) NaSCN, DMF, 140 °C, 59%; (c) NaOH, water/THF/EtOH, rt, quant.; (d) $(COCl)_2$, cat. DMF, THF, then aq. NH_3, 98% in 2 steps; (e) $POCl_3$, imidazole, pyridine, 67%.

Scheme 3. Synthesis of various 8-methylsulfanyl-4,5-dihydro-1*H*-thieno[3,4-*g*]isothiazole derivatives functionalized at the *N*-carboxamide moiety.

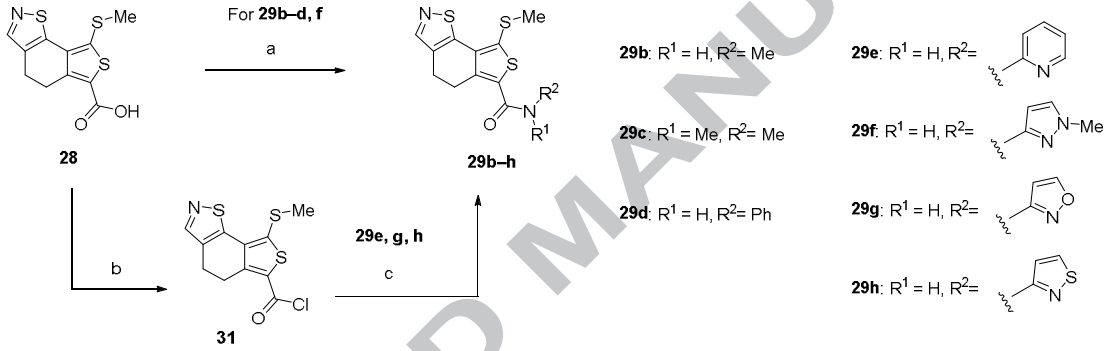

[a]Reagents and conditions: (a) HNR^1R^2, NMM, HATU, DMF, rt, 36–76%; (b) $SOCl_2$, toluene, rt, 67%: (c) HNR^1R^2, LiHMDS, THF, –20 °C, 19–42%.

The synthesis of various 8-substituted-4,5-dihydro-1*H*-thieno[3,4-*g*]isothiazole derivatives is shown in Scheme 4. Sulfoxide **32** and sulfone **33** were synthesized separately by oxidation of sulfide **29a** with the appropriate number of equivalents of mCPBA. For preparation of the final 8-aryloxy-4,5-dihydro-1*H*-thieno[3,4-*g*]isothiazole derivatives, S_NAr reaction of sulfone **33** with phenol in the presence of Cs_2CO_3 afforded desired product **34b** in only 10% yield. On the other hand, it was previously reported that the S_NAr reaction of bicyclic 4,5,6,7-tetrahydro-3-methylsulfonyl-4-oxobenzo[*c*]thiophene derivative **35** successfully provided aryl ether derivatives.[36a_b] In fact, nucleophilic addition was successfully employed to prepare **34b** by treatment of **35** with phenol in the presence of K_2CO_3 in 88% yield. The reason for this substantial improvement in yield is likely due to the improved electrophilicity of the bicyclic 4,5,6,7-tetrahydro-3-methylsulfonyl-4-oxobenzo[*c*]thiophene intermediate relative to the tricyclic 4,5-dihydro-1*H*-thieno[3,4-*g*]isothiazole intermediate. These findings led us to the facile preparation of a wide variety of 8-aryloxy-4,5-dihydro-1*H*-thieno[3,4-*g*]isothiazole derivatives **34a–i**. Introduction of the isothiazole ring into **36a–h**, followed by transformation of the ethyl ester group to a carboxamide group

was accomplished using the same method shown in Scheme 2 to afford derivatives **34a**–**h**. Oxidation of **34e** with mCPBA gave *N*-oxypyridine analog **34i** in good yield.

Scheme 4. Synthesis of various 8-substituted-4,5-dihydro-1*H*-thieno[3,4-*g*]isothiazole derivatives.

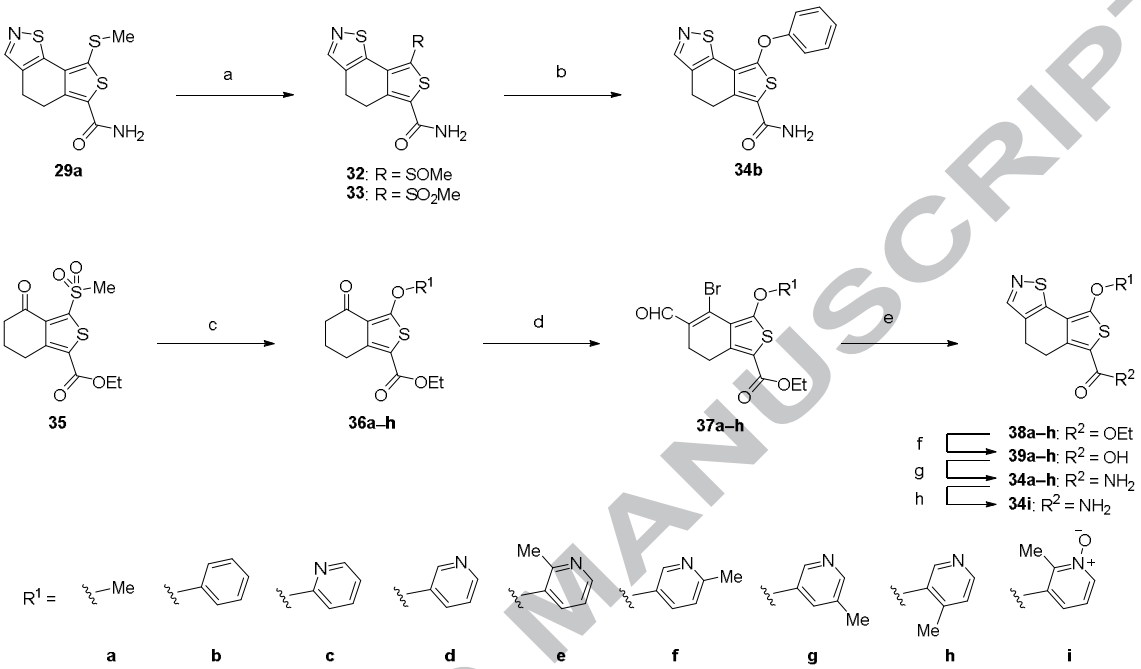

[a]Reagents and conditions: (a) mCPBA, DMF, rt, 55% for **32**, 49% for **33**; (b) phenol, Cs_2CO_3, NMP, 140 °C, 10%; (c) aryl alcohol, K_2CO_3, toluene/EtOAc, 80 °C, 16–95%; (d) PBr_3, DMF, CH_2Cl_2 or CH_3CN or DMF, 80 °C; (e) ammonium thioacetate, acetone or CH_3CN, 55 °C, 17–79% in 2 steps; (f) KOTMS, THF, rt; or aq. NaOH, THF/EtOH (or MeOH), rt, 70–97%; (g) NH_4OH, HOBt, WSC·HCl, DMF, rt; or $(COCl)_2$, DMF, THF, rt, then NH_4OH, 0 °C, 17–79%; (h) mCPBA, DMF, rt, 72%.

The synthesis of various 8-(pyridin-2-yloxy)-4,5-dihydro-1*H*-thieno[3,4-*g*]isothiazole derivatives was accomplished by Pd-catalyzed coupling as the key reaction (Scheme 5). Bromo analogs **44**, **45** and **47** as key intermediates were synthesized in a similar manner to that shown in Scheme 4. A carbon monoxide-free, Pd-catalyzed Heck aminocarbonylation[40] reaction of **47** employing the Herrmann-Beller palladacycle catalyst in conjunction with $Mo(CO)_6$ as a solid CO source in the presence of DBU[41] successfully provided a variety of *N*-substituted-6-carboxamide-3-oxy-pyridine derivatives **52e**–**f**. The Pd-catalyzed Heck carbonylation[42] of **47** with $Pd(OAc)_2$ and dppf catalyst in the presence of MeOH under CO atmosphere gave methyl ester intermediate **52l** in 64% yield. The transformation of methyl ester **52l** to primary amide **52d** was conducted by hydrolysis with aqueous NaOH, followed by the condensation with HOBt·NH_3 and WSC.

Scheme 5. The synthesis of substituted 8-(pyridin-2-yloxy)-4,5-dihydro-1*H*-thieno[3,4-g]isothiazole derivatives.

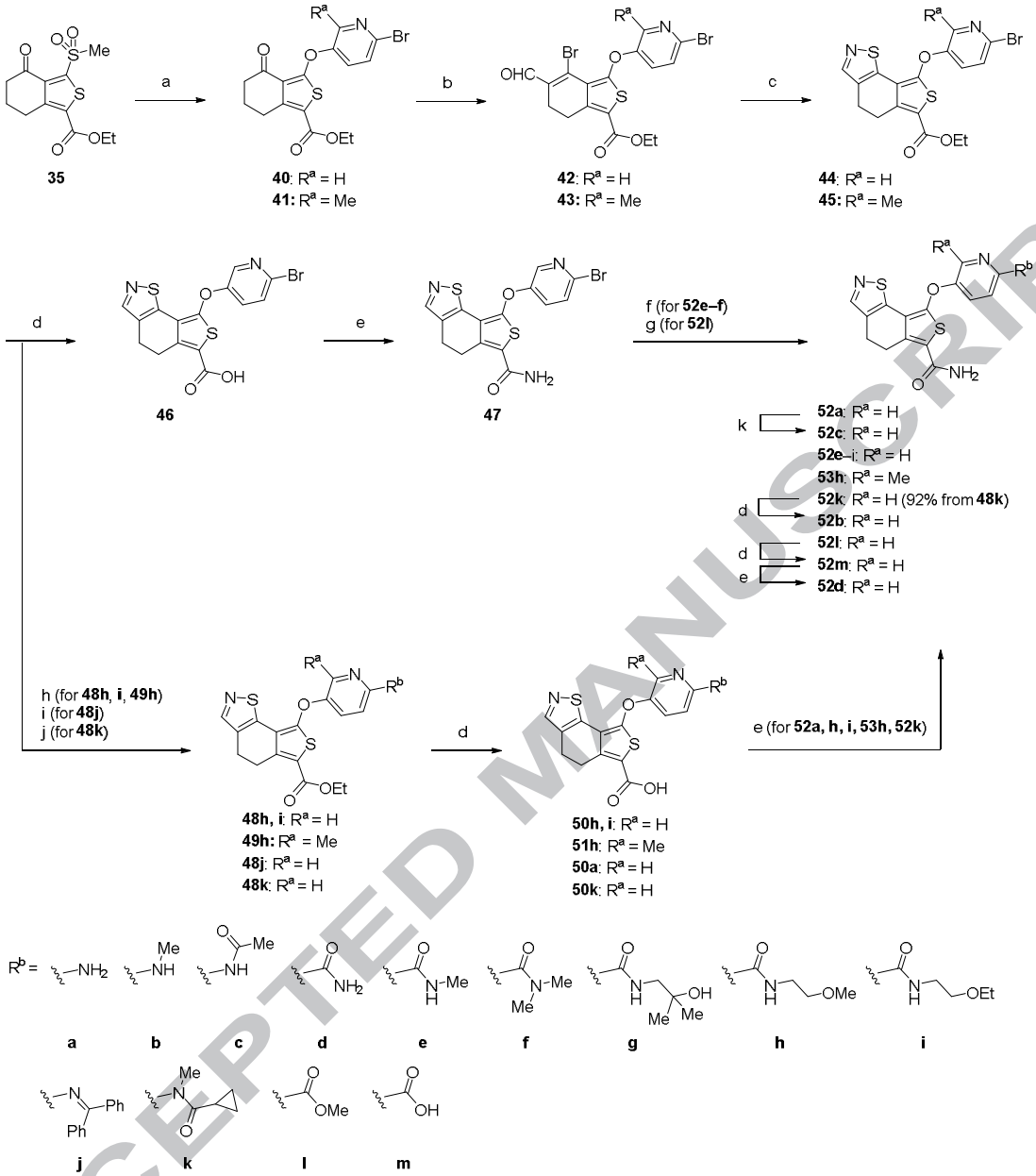

[a]Reagents and conditions: (a) aryl alcohol, K_2CO_3, toluene/EtOAc, 80 °C, 68%; (b) PBr_3, DMF, 80 °C, 83%; (c) ammonium thioacetate, acetone, 55–60 °C, 85%; (d) aqueous NaOH, THF/EtOH, rt, 55–100%; (e) NH_4OH and HOBt or HOBt·NH_3, WSC·HCl, DMF, rt, 47-100%; (f) amine, Herrmann-Beller palladacycle catalyst, $Mo(CO)_6$, DBU, THF, 125 °C, microwave, 36-75%; (g) MeOH, $Pd(OAc)_2$, dppf, NEt_3, DMF, 70 °C, CO_2 atmosphere, 3 atm, 64%; (h) amine, $(PPh_3)_2PdCl_2$, NEt_3, DMA, 80 °C, CO_2 atmosphere, 1 atm, 68–75%; (i) diphenylmethanimine, $Pd_2(dba)_3$, t-BuXPhos, NaOtBu, toluene, 60 °C, 47%; (j) *N*-methylcyclopropylamide, $Pd_2(dba)_3$, XPhos, toluene, 80 °C, 20%; (k) AcCl, DMA, rt, 33%.

Other *N*-substituted-6-carboxamide-3-oxy-pyridine derivatives **52a**, **52h**, **52i**, and **53h** were synthesized using an alternative route. The Pd-catalyzed Heck aminocarbonylation of **44** or **45** with

$(PPh_3)_2PdCl_2$ catalyst in the presence of Et_3N under CO atmosphere successfully provided various *N*-substituted-6-carboxamide-3-oxy-pyridine derivatives **48h–i**, **49h**. Transformation of the ethyl ester moiety of **48h–i**, **49h** to a carboxamide group by an analogous method to that shown in Scheme 3 afforded the desired compounds **52h–i** and **53h**. *N*-Substituted-6-amino-3-oxy-pyridine derivatives **52a–c** were synthesized using ethyl ester intermediate **44**. The Pd-Catalyzed Buchwald–Hartwig amination[42,43] of **44** and diphenylmethanimine with $Pd_2(dba)_3$ and t-BuXPhos afforded **48j** in 47% yield. Hydrolysis of **48j** with aqueous NaOH achieved double hydrolysis of both the ethyl ester and the imine group to afford 6-amino-3-oxy-pyridine compound **50a**. Transformation of the carboxylic acid group of **50a** to a carboxamide group in a manner similar to Scheme 3 provided **52a**, which was in turn acetylated to provide 6-acetylamino-3-oxy-pyridine derivative **52c**. On the other hand, conducting the analogous Pd-Catalyzed Buchwald–Hartwig amidation[43,44] of **44** with *N*-methylcyclopropylamide with $Pd_2(dba)_3$ and t-BuXPhos afforded **48k** in low yield (20%). Subsequent transformation of the ethyl ester moiety of **48k** to a carboxamide in a similar manner to that described above afforded **50k**. The hydrolysis of *N*-methy-*N*-cyclopropylamide group (**50k**) afforded 6-methylamino-3-oxy-pyridine derivative **52b**.

3. Results and discussion

3.1. In vitro biological evaluation

To discover novel, potent CDK8/19 dual inhibitors, novel [5,6,5]-fused tricyclic derivatives were evaluated in a ligand displacement assay against CDK8 and CDK19 kinases. In-cell western assay was used to assess the phosphorylation level of a direct downstream substrate of CDK8, STAT1 (pSTAT1), in SW480 cells.

Biological activity data for several [5,6,5]-fused tricyclic derivatives with different heterocycles in the A-ring position are shown in Table 1. Initial lead compound **16** showed good potency against CDK8 and CDK19, with IC_{50} values of 18 and 19 nM, respectively. The docking model of compound **16** bound to CDK8 suggested that a nitrogen atom at the N-2 position of the tricyclic scaffold forms a hydrogen bond with $^{+}NH_3$ of Lys52. Therefore, we examined the SAR for the introduction of other 5-membered heterocyclic rings in place of the A-ring with library compounds **16**, **54**, **55**, and **56**. Changing placement of the methyl group from the N-1 position (**16**) to the N-2 position (**54**), and removal of the methyl group (**55**) dramatically decreased binding potency. On the other hand, isoxazole compound **56** showed slightly decreased binding potency compared with imidazole **16**. These results are consistent with those of our modeling studies, suggesting that the lone pair of electrons at the N-2 nitrogen, along with hydrophobic interactions, are important for binding activity. As examples of more hydrophobic 5-membered heterocyclic rings with an electron lone pair at the N-2 position, isoxazole isothiazole compound **29a** was designed and evaluated. Isothiazole is a more hydrophobic heterocyclic ring than either imidazole or isoxazole. In fact, isothiazole compound **29a** showed dramatically increased binding activity against CDK8/19 with IC_{50} values of 0.65 and 1.3 nM, respectively. The introduction of an additional nitrogen atom at the 4-position, resulting in thiadiazole derivative **24**, resulted in somewhat diminished

potency along with increased hydrophilicities. Generally good correlation was found for this series of compounds between the CDK8 cell free binding activity and cellular activity, measured in terms of STAT1 phosphorylation. Thus, compound **29a** demonstrated high inhibitory activity in cell with an IC_{50} of 8.9 nM. Thus, we chose to focus on the 4,5-dihydrothieno[3',4':3,4]benzo[1,2-*d*]isothiazole scaffold for further efforts in the discovery of CDK8/19 dual inhibitors.

Table 1. Structure–activity relationships at the A-ring.

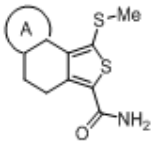

Compound	A	CDK8[a] IC_{50} (nM)	CDK19[a] IC_{50} (nM)	pSTAT1[a, b] EC_{50} (nM)
16	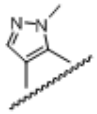	18 (13–24)	19 (15-24)	25 (16–39)
54	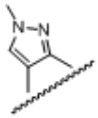	>10000	ND	>10000
55	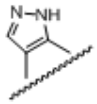	1700 (1200–2300)	3100 (2200-4400)	1300 (680–2300)
56	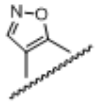	45 (39–52)	71 (58-88)	200 (130–320)
29a	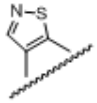	0.65 (0.39–1.1)	1.3 (0.76-2.2)	8.9 (4.2–19)
24	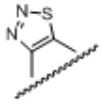	60 (43–83)	130 (78-220)	550 (200–1500)

[a] n = 2. Values in parentheses indicate 95% confidence interval. [b]Concentration producing 50% inhibition (EC50) values against CDK8 substrate STAT1 phosphorylation in SW480 cultured human colon cancer cell lines.

Next, we investigated the effect of introducing R groups with the potential to interact with the backbone C=O and NH of Ala100 in the kinase hinge region of CDK8; the results are summarized in Table

2. Initially, various alternative functional groups with hydrogen acceptor functionality were examined as potential replacements for the carboxamide moiety (**29a**), such as a carboxyl group (**28**) or nitrile (**30**). However, both modifications resulted in decreasing binding activity. Based on these results, we focused on *N*-substituted carboxamide derivatives. Compounds with increasing substitution at this position, such as *N*-methyl (**29b**), *N,N*-dimethyl (**29c**), *N*-phenyl (**29d**), showed diminished potency. Because the introduction of R groups at this position would place them in proximity to the hinge region, according to our CDK8 model, bulky groups might be expected to be unfavorable for binding affinity. On the other hand, the introduction of a 2-pyridyl group (**29e**) as the *N*-substituent showed weak binding activity. According to our modeling studies, the nitrogen atom of the 2-pyridyl ring might be able to interact with Alg365 in the kinase hinge region. Replacement of the 2-pyridyl ring with smaller 5-membered heteroaryl rings, such N-methylimidazole (**29f**) or isoxazole (**29g**), resulted in a dramatic recovery of enzymatic potency. On the other hand, isothiazole derivative **29h** showed decreased binding activity. Thus, our designs aimed at increasing interaction with Alg365 in the kinase hinge region led us to discover compound **29g**, possessing an *N*-3-oxazolo-aminocarbonyl group as a novel hinge binding moiety, with IC_{50} values of 12 nM and 15 nM against CDK8 and CDK19, respectively. However, compound **29g** still showed lower potency than lead compound **29a** bearing an unsubstituted carboxamide group.

Table 2. Structure–activity relationships around the carboxamide group

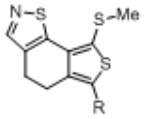

Compound	R	CDK8[a] IC_{50} (nM)	CDK19[a] IC_{50} (nM)	pSTAT1[a,b] EC_{50} (nM)
29a	$CONH_2$	0.65 (0.39–1.1)	1.3 (0.76-2.2)	8.9 (4.2–19)
28	CO_2H	9.5 (8.0–11)	12 (7.3–19)	>10000
30	CN	23 (11–48)	46 (20–103)	490 (280–860)
29b	CONHMe	9.3 (4.6–19)	22 (9.9–48)	140 (88–240)
29c	$CONMe_2$	68 (49–94)	120 (85–167)	1700 (690–4200)
29d	CONHPh	540 (410–700)	700 (480–1000)	>10000
29e	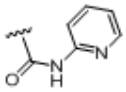	180 (120–290)	400 (150–640)	2800 (1100–6700)
29f	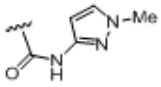	22 (16–31)	65 (49–87)	1400 (760–2600)
29g	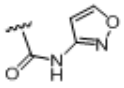	12 (6.9–22)	15 (6.6–36)	890 (440–1800)
29h	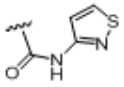	66 (47–92)	93 (60–150)	620 (380–1000)

[a] n = 2. Values in parentheses indicate the 95% confidence interval. [b]Concentration producing 50% inhibition (EC50) values for STAT1 phosphorylation in SW480 cultured human colon cancer cells.

Because **29a** showed sufficient in vitro potency to act as a CDK8/19 dual kinase inhibitor, the ADME properties of this compound were evaluated. Compound **29a** showed poor metabolic stability in

human liver microsomes, with a metabolic clearance value of 137 μL/min/mg (Table 3). To improve the metabolic stability of this series, we focused on reducing overall molecular lipophilicity to reduce compound recognition by metabolizing enzymes.[45] Oxidized sulfide analogs such as methyl sulfoxide (**32**) or methyl sulfone (**33**) derivatives, with lower cLogP values than methyl sulfide compound **29a**, were synthesized and tested. These compounds showed excellent metabolic stability, but also exhibited reduced in vitro potency. Replacement of the methylthio moiety of **29a** with a methoxy group (**34a**) resulted in an acceptable lipohilicity profile, with a cLogP value of 1.89, and recovered in vitro potency. However, the metabolic stability of **34a** could not be measured due to analytical issues. On the other hand, the results of our modeling studies suggested that there should be sufficient space in the hydrophobic front pocket region around the 8-position of 4,5-dihydrothieno[3',4':3,4]benzo[1,2-*d*]isothiazole scaffold to introduce a bulkier functional groups than methoxy. Therefore, we designed phenoxy derivative **34b**, which demonstrated comparable enzymatic potency to compound **29a**, albeit with decreased metabolic stability likely due to a high ClogP value of 3.88. Furthermore, **34b** demonstrated the most potent cellular activity among these derivatives, with an EC_{50} value of 0.77 nM. These results indicated that the introduction of a lipophilic front pocket moiety could be effectively employed to increase CDK8 inhibitory activity in cells. To further explore this possibility, we introduced pyridyloxy groups such as 2-pyridyloxy (**34c**) or 3-pyridyloxy (**34d**) (the corresponding 4-pyridyloxy derivative could not be obtained by the same S_NAr reaction shown in Scheme 5). Both compounds exhibited increased metabolic stability, along with a reduction in cLogP compared with **34b**. In particular, 3-pyridyloxy derivative (**34d**) exhibited potent enzymatic activity against CDK8 and CDK19 with IC_{50} values of 1.5 and 2.7 nM, respectively, and cellular activity with an IC_{50} value of 3.0 nM. Next, we explored the possibility of introducing functional groups into the pyridyl ring of 3-pyridyloxy derivative **34d**; initially, we examined the introduction of a methyl group into each position. Among the four methyl derivatives (**34e**–**h**) thus prepared, the 3-(2-methyl-pyridyloxy) (**34e**) and 3-(6-methyl-pyridyloxy) (**34f**) derivatives showed slightly increased enzymatic potency. Transformation to *N*-oxy-pyridyloxy derivative **34i** showed excellent metabolic stability with a significant reduction in cLogP to 1.00, but exhibited reduced potency. Based on these results, we focused further optimization efforts for 3-pyridyloxy derivatives on substitutions at the 2- or 6-positions, with a goal of delicately tuning the lipophilic properties of this series to obtain an appropriate balance of potency and metabolic stability.

Table 3. Structure–activity relationships at the 8-position of 4,5-dihydrothieno[3',4':3,4]benzo[1,2-d] isothiazole derivatives

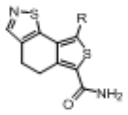

Compound	R	CDK8[a] IC_{50} (nM)	CDK19[a] IC_{50} (nM)	pSTAT1[a, b] EC_{50} (nM)	Metabolic Clearance[c] (μL/min/mg)	cLogP[d]
29a	SMe	0.65 (0.39–1.1)	1.3 (0.76–2.2)	8.9 (4.2–19)	137	2.39
32	SOMe	88 (67–120)	150 (110–190)	70 (38–130)	−12	0.67
33	SO_2Me	63 (54–74)	110 (92–130)	220 (120–380)	−4	0.63
34a	OMe	2.3 (1.5–3.3)	2.8 (1.7–4.7)	9.1 (6.1–14)	ND[e]	1.89
34b		0.34 (0.26–0.44)	0.55 (0.41–0.75)	0.77 (0.53–1.1)	193	3.88
34c		11 (6.1–18)	25 (12–52)	66 (31–140)	101	2.38
34d		1.5 (1.1–2.2)	2.7 (1.8–4.0)	3.0 (1.9–4.6)	55	2.38
34e		0.47 (0.67–1.5)	0.77 (0.53–1.1)	2.0 (0.95–4.3)	86	2.88
34f	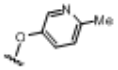	0.99 (0.67–1.5)	1.3 (0.93–1.7)	3.00 (2.0–4.5)	75	2.88
34g	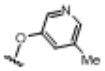	5.1 (4.1–6.8)	9.2 (7.6–11)	28 (19–40)	188	2.88
34h		4.7 (3.3–6.8)	6.6 (4.7–9.1)	16 (8.6–31)	65	2.88
34i		4.4 (3.3–5.8)	9.3 (7.8–11)	8.3 (5.2–13)	−5	1.00

[a] n = 2. Values in parentheses indicate the 95% confidence interval. [b] Concentration producing 50% inhibition (EC50) values for STAT1 phosphorylation in SW480 cultured human colon cancer cells. [c] Metabolic clearance measured using human liver microsomes and NADPH. [d] cLogP was calculated by Daylight Software. [e] Not determined.

Further substituted 3-pyridyloxy derivatives (**52a–i**, **53h**) were prepared and evaluated, as shown in Table 4. Initially, we examined 3-pyridyloxy derivatives including mono-substitution at the pyridine 6-position, which were more easily synthesized than modifications at the 2-position. To improve metabolic stability, replacements of methyl with more hydrophilic functional groups were examined. The 3-(6-amino-pyridyloxy) derivative **52a** showed significantly improved human metabolic stability (30 μL/min/mg), while maintaining in vitro potency. However, compound **52a** showed poor solubility in aqueous solutions under neutral conditions (pH 6.8), with a solubility value of 4.5 μg/mL. The introduction of the further functional groups into the amino moiety of **52a**, such as methyl group (**52b**) or acetyl group (**52c**), decreased metabolic stability. On the other hand, preparation of aminocarbonyl compound **52d** significantly reduced the molecular lipophilicity (cLogP: 1.88) and improved metabolic stability, while maintaining in vitro enzymatic potency and cellular activity. However, compound **52d** also showed poor aqueous solubility. Based on these results, we examined the possibility of extending the functional group with more flexible substituents to improve aqueous solubility while maintaining good metabolic stability. To confirm our hypothesis, we prepared *N*-methylaminocarbonyl derivative **52e** and *N,N*-dimethylaminocarbonyl derivative **52f**. Monomethyl derivative **52e** showed improved aqueous solubility with high in vitro potency and good metabolic stability; dimethyl derivative **52f** demonstrated dramatically improved aqueous solubility with good metabolic stability, but showed slightly reduced in vitro potency. These results led us to continue studies of *N*-methylaminocarbonyl derivatives. Among a variety of compounds prepared by parallel synthesis, we found that *N*-(2-methoxyethyl)-aminocarbonyl derivative **52h** showed excellent metabolic stability and aqueous solubility. Furthermore, **52h** maintained enzyme inhibitory activity against CDK8 and CDK19 (IC_{50}: 0.46 nM and 0.99 nM, respectively), and demonstrated enhanced cellular potency relative to **34f** with an EC_{50} value of 1.3 nM. The introduction of an additional methyl group into the pyridyl 2-position (**53h**) or a methoxyethyl moiety into the amide functionality (**52i**) dramatically reduced metabolic stability likely due to high cLogP values, as well as aqueous solubility. Therefore, we selected **52h** as a promising compound with sufficient in vitro potency and physicochemical properties for further in-depth evaluation.

Table 4. Structure–activity relationships of 3-pyridyloxy derivatives.

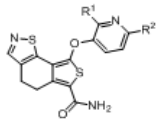

Compound	R^1	R^2	CDK8[a] IC_{50} (nM)	CDK19[a] IC_{50} (nM)	pSTAT1[a, b] EC_{50} (nM)	Metabolic Clearance[c] (μL/min/mg)	Solubility[e] pH6.8 (μg/mL)	cLogP[d]
34f	H	Me	0.99 (0.67–1.5)	1.3 (0.93–1.7)	3.0 (2.0–4.5)	75	23	2.88
52a	H	NH_2	0.60 (0.43–0.85)	1.1 (0.78–1.6)	2.3 (1.4–3.8)	30	4.5	2.06
52b	H		0.59 (0.28–1.2)	0.36 (0.17–0.75)	0.58 (0.42–0.82)	127	4	2.86
52c	H		0.57 (0.46–0.70)	0.57 (0.43–0.75)	0.40 (0.26–0.62)	61	0.72	2.23
52d	H		0.93 (0.77–1.1)	0.97 (0.69–1.4)	1.4 (0.97–2.0)	19	4.1	1.88
52e	H		1.9 (1.6–2.2)	1.0 (0.83–1.3)	2.6 (1.1–6.2)	23	11	2.20
52f	H		23 (14–36)	21 (17–26)	21 (14–31)	36	65	1.25
52g	H	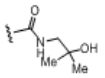	2.4 (1.6–3.6)	2.4 (1.9–3.2)	7.4 (3.7–14)	21	56	2.34
52h	H	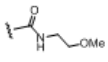	0.46 (0.37–0.56)	0.99 (0.77–1.3)	1.3 (0.74–2.2)	21	47	2.40
52i	H	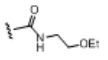	1.1 (0.99–1.2)	1.9 (1.7–2.2)	1.5 (0.99–2.3)	73	15	2.79
53h	Me	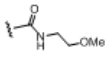	1.4 (1.0–1.8)	1.3 (1.1–1.5)	0.35 (0.23–0.53)	71	6.7	2.90

[a] n = 2. Values in parentheses indicate the 95% confidence interval. [b]Concentration producing 50% inhibition (EC50) values for STAT1 phosphorylation in SW480 cultured human colon cancer cells. [c]Metabolic clearance measured using human liver microsomes and NADPH. [d]cLogP was calculated by Daylight Software. [e]10 mmol/L solution of the compound in DMSO was evaluated using JP2 buffer (pH 6.8), as described in the Japanese Pharmacopoeia. [e]Not determined.

3.2. Kinase inhibitory profiles of 29a and 52h.

The in vitro kinase inhibitory activity of **29a** and **52h** was assessed against a panel of 27 kinases. A listing of IC_{50} values for those kinases that were inhibited more than 50% at 1.0 μM compound concentration by at least one of the compounds tested is shown in Table 5. Methyl sulfide compound **29a** showed multiple kinase inhibitory activities. On the other hand, pyridyl ether compound **52h** exhibited dramatically more selective kinase activity, and enzyme inhibitory activity against only CDK family

kinases (IC_{50} values of 0.99 nM for CDK19, 62% inhibition at 1 μM for CDK2, 270 nM for CDK9). Furthermore, the inhibitory activity of **52h** against CDK2 was significantly less potent than that against CDK8. The origin of such high selectivity is suggested in a general sense by the data shown Table 6, which outlines variations in amino acid residues found across the kinase family in the DXG loop and gatekeeper regions. CDK8 and CDK19 are somewhat rare examples, among CDK family proteins as well as the general kinase family, of kinases that possess a Met residue in the DXG activation loop and a Phe residue as the gatekeeper. In our comparison of kinase selectivity for **29a** and **52h**, the kinases that show a dramatic reduction of inhibitory activity for **52h** (GSK3β, PLK1, ASK1, CK1δ, PKA, ROCK1, PKCθ, CDC7) are all kinases that differ from CDK8/19 in the amino acid residues found in the DXG motif and gatekeeper. CDK2 and CDK9 do each possess a Phe gatekeeper residue, but differ from CDK8/19 in the DXG loop (X = Phe), which could explain some residual but diminished inhibitory activity for these kinases. A docking study of **52h** bound to CDK8 suggested that the tricyclic scaffold interacts with the Phe gatekeeper, with the pyridyl ether moiety locates near the Met residue in the DMG motif of CDK8 kinase (Figure 5). Based on these results, we reason that the scaffold itself, combined with the introduction of the pyridyl ether sidechain result in the high kinase specificity found for **52h** with respect to the CDK8 and CDK19 kinases.

Compound **52h** was further tested against a panel of 456 kinases in a panel binding assay (KINOMEscan™ from DiscoveRx Corp.)[46] to determine its selectivity (Figure 6.(a)). At a concentration of 300 nM, the percent of unbound compound **52h** was 8.3% for CDK8 and 4.6% for CDK19, with HASPIN (23%), DYRK1B (27%), and HIP1 (32%) being the kinases with the next highest binding affinity. Only 10 kinases showed <50% unbound fraction at 300 nM (YSK4: 41%, EPHA3: 43%, DYRK1A: 47%, HIPK2: 48%, IRK1: 49%), and full K_d curves were measured for seven of these (Figure 6.(b)).

Table 5. Kinase selectivity of **29a** and **52h**.[a]

Kinase[c]	%inhibition at 1 μM	
	29a	**52h**
CDK8	99 (IC_{50} = 0.65 nM)	105 (IC_{50} = 0.46 nM)
CDK19	97 (IC_{50} = 1.7 nM)	100 (IC_{50} = 0.99 nM)
CDK2	95	62
CDK9	105 (IC_{50} = 4.0 nM)	83 (IC_{50} = 270 nM)
GSK3β	64	31
PLK1	62	4
ASK1	60	0
CK1δ	94	28
PKA	62	1
ROCK1	81	7
PKCθ	77	2
CDC7	91	33

[a]No significant inhibition observed at concentrations <1 μM for the following kinases: AKT1 (v-akt murine thymoma viral oncogene homolog 1), Aurora B (aurora kinase A), MEK1 (mitogen-activated protein kinase kinase 1), MAPKAPK2 (mitogen-activated protein kinase-activated protein kinase 2), CHK1 (checkpoint kinase 1), EGFR (epidermal growth factor receptor), VEGFR2 (vascular endothelial growth factor receptor 2), cMET (met proto-oncogene), EPHA5 (ephrin type-A receptor 5 precursor), JAK1 (janus kinases 1), FAK (focal adhesion kinase), SRC (v-src sarcoma), IRK (insulin receptor kinase), PI3Kα (phosphoinositide 3-kinase α), ERK1 (extracellular signal-regulated kinase 1), p38α (mitogen-activated protein kinase 14), TrkA (neurotrophic tyrosine kinase, receptor, type 1). [b]n = 2. [c]GSK3β (glycogen synthase kinase 3β), PLK1 (polo-like kinase 1), ASK1 (Apoptosis signal-regulating kinase 1), CK1δ (casein kinase 1δ), PKA (protein kinases-A), ROCK1 (rho-associated protein kinase 1), PKCθ (protein kinase Cθ), CDC7 (cell division cycle 7).

Table 6. Analysis of amino acid residues found in DXG motif and gatekeeper for kinase family proteins.

Kinase	DXG motif	Gatekeeper
	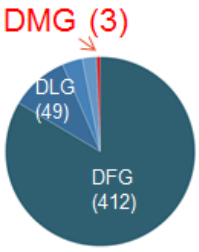	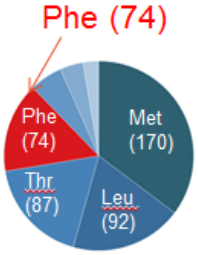
	(reported 493 of 497 human kinases)	(reported 482 of 497 human kinases)
CDK8, CDK19	Met	Phe
CDK2, CDK9	Phe	Phe
GSK3β, PLK1	Phe	Leu
ASK1, CK1δ, PKA, ROCK1, PKCθ, CDC7	Phe	Met

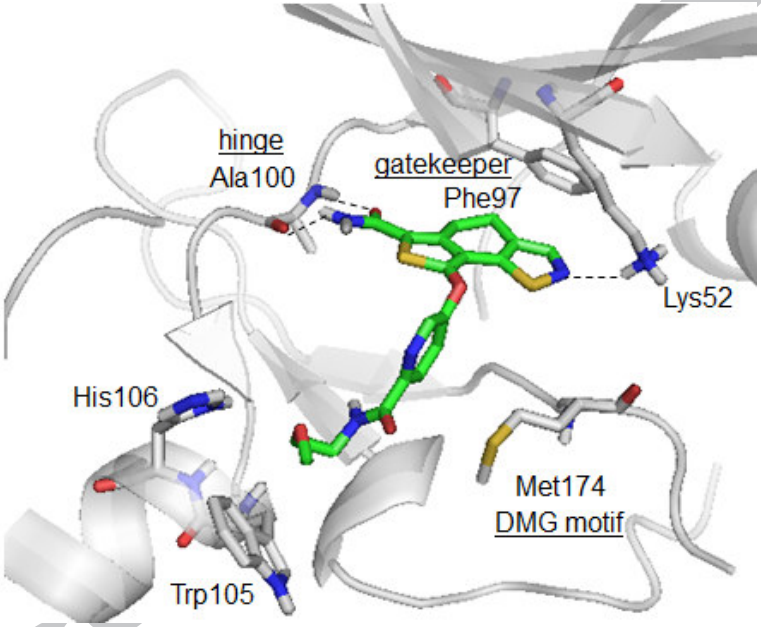

Figure 5. Docking model of **52h** bound to CDK8.

(a)

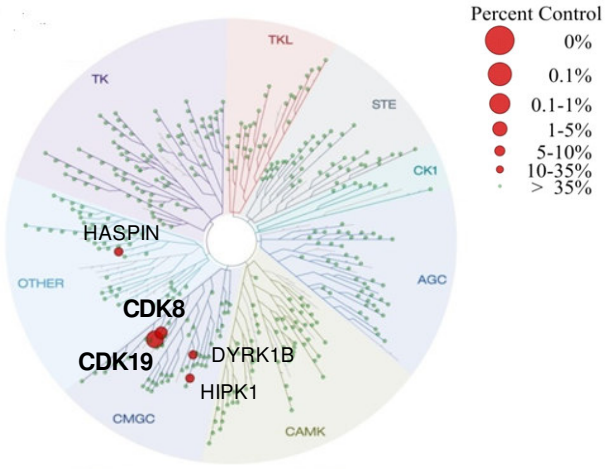

(b)

Kinase	K_d (nM)
CDK19	25
CDK8	46
DYRK1B	81
HASPIN	86
YSK4	97
HIPK1	160
EPHA3	>3000

Figure 6. (a) Selectivity profile of 52h at 300 nM against 456 kinases (evaluated by KINOME*scan*™ profiling). Percent relative to control (unbound fraction) for each kinase is depicted by the size of the red circle. (b) K_d values for kinases with most potent binding affinity shown. DYRK1B (Dual specificity tyrosine-phosphorylation-regulated kinase 1A), DYRK1B (Dual specificity tyrosine-phosphorylation-regulated kinase 1B), EPHA3 (ephrin type-A receptor 3), HASPIN (GSG2: germ cell assiciated 2), HIPK1 (Homeodomain-interacting protein kinase 1), IRK1 (Interleukin-1 receptor-associated kinase 1), YSK4 (Sps1/Ste20-related kinase homolog).

3.3. In vitro pharmacology of 52h.

To evaluate the anti-proliferative activity of **52h** against cancer cells, we measured inhibitory activity against phosphorylation of STAT1, a direct substrate of CDK8, as well as cell growth inhibitory activity in vitro (Table 7). In several types of colon, multiple myeloma, acute myelogenous leukemia (AML), lung cancer cells, **52h** suppressed phospho-STAT1 levels. **52h** also demonstrated anti-proliferative activities among these cell lines with GI_{50} of 0.43–2.5 nM, with the exception of the SW480 cell line. GI_{50} was not determined in SW480 cells because **52h** did not suppress SW480 cell growth to a level below 50%. Based on these and other results, we have found that phospho-STAT1 is an appropriate target engagement marker, which is suppressed by **52h** in all of cell lines, but does not always reflect sensitivity of cell growth in the cell lines. A sensitivity prediction marker for cell growth inhibition is under investigation and will be published in the near future.

Table 7. STAT1 suppression effect by 1 day treatment of **52h** (Western blotting: WB) and its anti-proliferative activity (GI_{50}) in various cancer cell lines.

Cell line	Organ	WB: Phospho-STAT1 0 3 30 (nM)	Cell Proliferation[a] GI_{50} (nM)
SW480	**Colon**	pS727-STAT1 STAT1 β-actine	–
RPMI8226	**Multiple Myeloma**	pS727-STAT1 STAT1 β-actine	2.5 (1.9–4.5)
MV-4-11	**AML**	pS727-STAT1 β-actine	1.6 (1.3–1.8)
Calu-1	**Lung**	pS727-STAT1 β-actine	0.43 (0.067–2.8)

[a]Cell proliferation determined by ATP content (SW480, RPMI8226 and MV-4-11) or nuclear count (Calu-1).

3.4. In vivo pharmacology of 52h.

Given its promising in vitro biological activity, a preliminary pharmacokinetic study of **52h** was conducted using cassette dosing in ICR mice. As shown in Table 8, compound **52h** displayed good pharmacokinetic properties, with an oral bioavailability of 98.5% and an in vivo half-life of 2.1 h. With sufficient oral bioavailability confirmed, we then proceeded to examine the in vivo antitumor efficacy of **52h** in a mouse xenograft model bearing RPMI8226 cells, which was one of the most sensitive cell lines in vitro (Table 8).

The antitumor efficacy and body weight loss of **52h** observed after oral administration of 1.25 mg/kg twice daily or 2.5 mg/kg once daily in an RPMI8226 human hematopoietic and lymphoid xenograft model in mice is shown Figure 7 (a). Compound **52h** showed tumor growth suppression with T/C of 27%, without severe body weight loss, two weeks after administration at a dose of 1.25 mg/kg. Furthermore, we observed tumor stasis with T/C of 1% two weeks after administration at a dose of 2.5 mg/kg for **52h**, accompanied by moderate body weight loss. We measured STAT1 phosphorylation levels in mouse blood as a PD maker, sampling 2 h and 8 h after the last administration (day 14) (Figure 7 (b)). Compound **52h** demonstrated decreased STAT1 phosphorylation levels at each time point for both doses. Based on these

results, we concluded that the tumor suppression observed for **52h** was caused by the inhibition of CDK8/19 activity.

Most tolerable dose (MTD) of compound **52h** is 2.5 mg/kg in SCID mouse model. We conducted the efficacy study at MTD and a half of MTD to evaluate the margin between efficacy and tolerability. The result suggests that **52h** effectively suppresses tumor growth with more than two-fold safety margin in mice.

Table 8. Pharmacokinetic parameters for **52h** in ICR mice.[a]

Dose (mg/kg)	Route	CL_{total} (mL h^{-1} kg^{-1})	V_{dss} (mL/kg)	MRT (h)	AUC_{0-24h} (μ g h/mL)	C_{max} po (μ g h/mL)	F (%)
0.1 mg	i.v.	1109 ± 69	2135 ± 107	1.93 ± 0.06	90.4 ± 5.5		
1 mg	p.o.			2.06 ± 0.23	890.9 ± 177.6	362.4 ± 85.8	98.5 ± 20.5

[a]Data are expressed as the mean ± SD (n = 3)

(a)

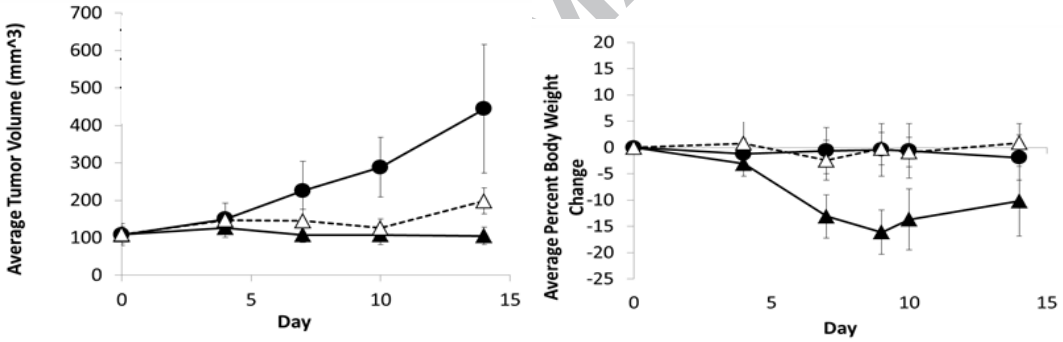

Legend		Dose (mg/kg)	*T/C* (%)	Body weight loss (%)
●	Vehicle		100	0
△	**52h**	1.25 b.i.d.	27[a]	−0.9
▲	**52h**	2.5 q.d.	−1[a]	−10.2

(b)

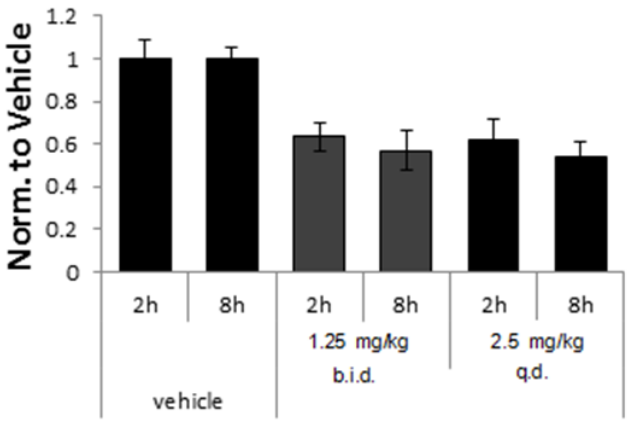

Figure 7. (a) Mean (n = 6) tumor volumes and body weights in nude mice bearing RPMI8226 human hematopoietic and lymphoid xenograft tumors dosed with **52h** or vehicle. $P \leq 0.05$ vs control at day 14 (Dunnett's t-test). (b) Mean (n = 6) phosphorylated STAT1 levels in nude mice bearing RPMI8226 human hematopoietic and lymphoid xenograft tumors 2 h and 8 h after the last administration (day 14) with a dose of 1.25 mg/kg, b.i.d., po or 2.5 mg/kg, q.d., po of **52h**.

4. Conclusion

We designed and developed CDK8/19 dual inhibitors bearing a novel 4,5-dihydrothieno[3',4':3,4]benzo[1,2-d]isothiazole scaffold utilizing structure-based drug design techniques based on docking models of our lead compound, 4,5-dihydroimidazolo[3',4':3,4]benzo[1,2-d]isothiazole **16** bound to CDK8. To improve physicochemical properties and kinase selectivity, we introduced a substituted 3-pyridyloxy group into the 8-position of the scaffold in the front pocket region. The resulting optimized compound **52h** showed excellent in vitro potency, physicochemical properties, and kinase selectivity. Based on our docking model of **52h** bound to CDK8, we could explain the highly specific kinase activity profile found for this compound, based on the interaction of the pyridyl ether sidechain of **52h** interacting with Met174 of the DMG activation loop of CDK8.

In vitro pharmacological evaluation of **52h** revealed potent suppression of phosphorylated STAT1 in various cancer cells. The high oral bioavailability found for this compound enabled in vivo studies, in which we demonstrated a mechanism-based in vivo PD effect as well as tumor growth suppression in an

RPMI8226 human hematopoietic and lymphoid xenograft model in mice. These results suggested that inhibition of CDK8/19 may provide strong antitumor efficacy and that **52h** is a promising candidate for the treatment of various human cancers. Further pharmacological evaluation of this compound and of CDK8/19 inhibition is in progress and will be reported in due course.

Acknowledgements

The authors thank Takashi Motoyaji and Akiyoshi Tani for target identification studies of compound **16**. We also would like to express our appreciation to Tsuneo Yasuma, Akira Mori, Hitoaki Nishikawa, Yoshihiro Banno, Jun Fujimoto, Abhijit Nayek, and Goutam Saha for their helpful advice and support in organic synthesis. We also thank Yukio Toyoda for his assistance in cell Western blotting assay development, and Tsuyoshi Ishii for his useful discussion about in vitro assay development. We are also grateful to Hiroshi Miyake, Hikichi Yuichi, and Tomoyasu Ishikawa for helpful discussion and guidance in the overall execution of this research.

Supplementary material

Supplementary data for experimental section associated with this article can be found, in the online version, at XXXXXX.

References and notes

1. For a representative review, see: Malumbres, M. *Genome Biol.* **2014**, *15*, 122.

2. For selected reviews, see: (a) Galons, H.; Oumata, N.; Gloulou, O.; Meijer, L. *Expert Opin. Ther. Patents* **2013**, *23*, 945–963; (b) Blachly, J. S.; Byrd, J. C. *Leuk. Lymphoma* **2013**, *54*, 2133–2143; (c) Mariaule, G.; Belmont, P. *Molecules* **2014**, *19*, 14366–14382; (d) Asghar, U.; Witkiewicz, A. K.; Turner, N. C.; Knudsen, E. S. *Nat. Rev. Drug Discov.* **2015**, *14*, 130–146; (e) Sánchez-Martínez, C.; Gelbert, L. M.; Lallena, M. J.; de Dios, A. *Bioorg. Med. Chem. Lett.* **2015**, *25*, 3420–3435; (f) Vymětalová, L.; Kryštof, V. *Med. Res. Rev.* **2015**, *35*, 1156–1174. (g) Malínková, V.; Vylíčil, J.; Kryštof, V. *Expert Opin. Ther. Patents* **2015**, *25*, 953–970; (h) Di Giovanni, C.; Novellino, E.; Chilin, A.; Lavecchia, A.; Marzaro, G. *Expert Opin. Investig. Drugs* **2016**, *25*, 1215–1230.

3. For selected reviews, see: (a) Romano, G.; Giordano, A. *Cell Cycle* **2008**, *7*, 3664–3668; (b) Kryštof,, V.; Uldrijan, S. *Curr. Drug. Targets* **2010**, *11*, 291–302; (c) Węsierska-Gądek, J.; Kramer, M. P. *Expert Opin. Investig. Drugs* **2011**, *20*, 1611–1628; (d) Fisher, R. P. *Genes Cancer* **2012**, *3*, 731–738; (e) Kryštof, V.; Baumli, S.; Fürst, R. *Curr. Pharm. Des.* **2012**, *18*, 2883–2890; (f) Bose, P.; Simmons, G. L.; Grant, S. *Expert Opin. Investig. Drugs* **2013**, *22*, 723–738; (g) Romano, G. *ISRN Oncol.* **2013**, *2013*, 305371; (h) Sonawane, Y. A.; Taylor, M. A.; Napoleon, J. V.; Rana, S.; Contreras, J. I.; Natarajan, A. *J. Med. Chem.* **2016**, *59*, 8667–8684; (i) Rahaman, M. H.; Kumarasiri, M.; Mekonnen, L.; Yu, M.; Diab, S.; Albrecht, H.; Milne, R. W.; Wang, S. *Endocr. Relat. Cancer* **2016**, ASAP.

4. For selected reviews, see: (a) Nemet, J.; Jelicic, B.; Rubelj, I.; Sopta, M. *Biochimine* **2014**, *97*, 22–27; (b) Rzymski, T.; Mikula, M.; Wiklik, K.; Brzózka, K. *Biochim. Biophys. Acta* **2015**, *1854*, 1617–1629; (c) Clark, A. D.; Oldenbroek, M.; Boyer, T. G. *Crit. Rev. Biochem. Mol. Biol.* **2015**, *50*, 393–426.

5. Firestein, R.; Shima, K.; Nosho, K.; Irahara, N.; Baba, Y.; Bojarski, E.; Giovannucci, E. L.; Hahn, W. C.; Fuchs, C. S.; Ogino, S. *Int. J. Cancer* **2010**, *126*, 2863–2873.

6. (a) Firestein, R.; Bass, A. J.; Kim, S. Y.; Dunn, I. F.; Silver, S. J.; Guney, I.; Freed, E.; Ligon, A. H.; Vena, N.; Ogino, S.; Chheda, M. G.; Tamayo, P.; Finn, S.; Shrestha, Y.; Boehm, J. S.; Jain, S.; Bojarski, E.; Mermel, C.; Barretina, J.; Chan, J. A.; Baselga, J.; Tabernero, J.; Root, D. E.; Fuchs, C. S.; Loda, M.; Shivdasani, R. A.; Meyerson, M.; Hahn, W. C. *Nature* **2008**, 455, 547–551; (b) Salari, K.; Spulak, M. E.; Cuff, J.; Forster, A. D.; Giacomini, C. P.; Huang, S.; Ko, M. E.; Lin, A. Y.; van de Rijn, M. Pollack, J. R. *Proc. Natl. Acad. Sci. USA* **2012**, *109*, E3196–E3205.

7. Yergiyev, O.; Garib, G.; Schoedel, K.; Palekar, A.; Bartlett, D.; Rao, U. N. *Appl. Immunohistochem. Mol. Morphol.* **2016**, ASAP.

8. Broude, E. V.; Győrffy, B.; Chumanevich, A. A.; Chen, M.; McDermott, M. S.; Shtutman, M.; Catroppo, J. F.; Roninson, I. B. *Curr. Cancer Drug Targets* **2015**, *15*, 739–749.

9. For selected reviews, see: (a) Taatjes, D. J. *Trens Biochem. Sci.* **2010**, *35*, 315–322; (b) Conaway, R. C; Conaway, J. W. *Curr. Opin. Genet. Dev.* **2011**, *21*, 225–230; (c) Conaway, R. C.; Conaway, J. W. *Semin. Cell Dev. Biol.* **2011**, *22*, 729–734; (d) Borggrefe, T.; Yue, X. *Semin. Cell Dev. Biol.* **2011**, *22*, 759–768; (e) Hentges, K. E. *Semin. Cell Dev. Biol.* **2011**, *22*, 769–775; (f) Napoli, C.; Sessa, M.; Infante, T.; Casamassimi, A. *Biochimie* **2012**, *94*, 579–587; (g) Conaway, R. C.; Conaway, J. W. *Biochim. Biophys. Acta* **2013**, *1829*, 69–75; (h) Ansari, S. A.; Morse, R. H. *Cell Mol. Life Sci.* **2013**, *70*, 2743–2756; (i) Carlsten, J. O. P.; Zhu, X.; Gustafsson, C. M. *Trends Biochem. Sci.* **2013**, *38*, 531–537; (j) Poss, Z. C.; Ebmeier, C. C.; Taatjes, D. J. *Crit. Rev. Biochem. Mol. Biol.* **2013**, *48*, 575–608; (k) Schiano, C.; Casamassimi, A.; Rienzo, M.; de Nigris, F.; Sommese, L.; Napoli, C. *Biochem. Biophys. Acta* **2014**, *1845*, 66–83; (l) Yin, J.-W.; Wang, G. *Development* **2014**, *141*, 977–987; (m) Allen, B. L.; Taatjes, D. J. *Nat. Rev. Mol. Cell Biol.* **2015**, *16*, 155–166.

10. (a) Pavri, R.; Lewis, B.; Kim, T.-K.; Dilworth, F. J.; Erdjument-Bromage, H.; Tempst, P.; de Murcia, G.; Evans, R.; Chambon, P.; Reinberg, D. *Mol. Cell* **2005**, 18, 83–96; (b) Knuesel, M. T.; Meyer, K. D.; Bernecky, C.; Taatjes, D. J. *Genes Dev.* **2009**, *23*, 439–451; (c) Galbraith, M. D.; Donner, A. J.; Espinosa, J. M. *Transcription* **2010**, *1*, 4–12; (d) Donner, A. J.; Ebmeier, C. C.; Taatjes, D. J.; Espinosa, J. M. *Nat. Struct. Mol. Biol.* **2010**, *17*, 194–201; (e) Takahashi, H.; Parmely, T.; Sato, S.; Tomomori-Sato, C.; Banks, C. A. S.; Kong, S. E.; Szutorisz, H.; Swanson, S. K.; Martin-Brown, S.; Washburn, M. P.; Florens, L.; Seidel, C. W.; Lin, C.; Smith, E. R.; Shilatifard, A.; Conaway, R. C.; Conaway, J. W. *Cell* **2011**, *146*, 92–104; (f) Galbraith, M. D.; Allen, M. A.; Bensard, C. L.; Wang, X.; Schwinn, M. K.; Qin, B.; Long, H. W.; Daniels, D. L.; Hahn, W. C.; Dowell, R. D.; Espinosa, J. M. *Cell* **2013**, *153*, 1327–1339.

11. (a) Meyer, K. D.; Donner, A. J.; Knuesel, M. T.; York, A. G.; Espinosa, J. M.; Taatjes, D. J. *EMBO J.* **2008**, *27*, 1447–1457; (b) Knuesel, M. T.; Meyer, K. D.; Donner, A. J.; Espinosa, J. M.; Taatjes, D. J. *Mol. Cell. Biol.* **2009**, *29*, 650–661; (c) Lai, F.; Orom, U. A.; Cesaroni, M.; Beringer, M.; Taatjes, D. J.; Blobel,

G. A.; Shiekhattar, R. *Nature* **2013**, *494*, 497–501.

12. (a) Morris, E. J.; Ji, J.-Y.; Yang, F.; Stefano, L. D.; Herr, A.; Moon, N.-S.; Kwon, E.-J.; Haigis, K. M. Näär, A. M.; Dyson, N. J. *Nature* **2008**, *455*, 552–556; (b) Tsutsui, T.; Fukasawa, R.; Tanaka, A.; Hirose, Y.; Ohkuma, Y. *Genes Cells* **2011**, *16*, 1208–1218; (c) Porter, D. C.; Farmaki, E.; Altilia, S.; Schools, G. P.; West, D. K.; Chen, M.; Chang, B.-D.; Puzyrev, A. T.; Lim, C.-U., Rokow-Kittell, R.; Friedhoff, L. T.; Papavassiliou, A. G.; Kalurupalle, S.; Hurteau, G.; Shi, J.; Baran, P. S.; Gyorffy, B.; Wentland, M. P.; Broude, E. V.; Kiraris, H.; Roninson, I. B. *Proc. Natl. Acad. USA* **2012**, *109*, 13799–13804; (d) Zhao, J.; Ramos, R.; Demma, M. *Oncogene* **2013**, *32*, 3520–3530; (e) Cai, W. S.; Shen, F.; Feng, Z.; Chen, J.-W.; Liu, Q.-C.; Li, E.-M.; Xu, B.; Cao, J. *Biomed. Pharmacother.* **2015**, *74*, 153–157; (f) Xu, W.; Wang, Z.; Zhang, W.; Qian, K.; Li, H.; Kong, D.; Li, Y.; Tang, Y. *Cancer Lett.* **2015**, *356*, 613–627.

13. (a) Bancerek, J.; Poss, Z. C.; Steinparzer, I.; Sedlyarov, V.; Pfaffenwimmer, T.; Mikulic, I.; Dölken, L.; Strobl, B.; Müller, M.; Taatjes, D. J.; Kovarik, P. *Immunity* **2013**, *38*, 250–262; (b) Putz, E. M.; Gotthardt, D.; Hoermann, G.; Csiszar, A.; Wirth, S.; Berger, A.; Straka, E.; Rigler, D.; Wallner, B.; Jamieson, A. M.; Pickl, W. F.; Zebedin-Brandl, E. M.; Müller, M.; Decker, T.; Sexl, V. *Cell Rep.* **2013**, *4*, 437–444; (c) Staab, J.; Herrmann-Lingen, C.; Meyer, T. *JAKSTAT* **2013**, *2*, e24275; (d) Putz, E. M.; Gotthaedt, D.; Sexl, V. *Oncoimmunology* **2014**, *3*, e955441.

14. (a) Fryer, C. J.; White, J. B.; Jones, K. A. *Mol. Cell* **2014**, *16*, 509–520; (b) Trakala, M.; Malumbres, M. *Nat. Cell Biol.* **2014**, *16*, 1031–1033; (c) Li, N.; Fassl, A.; Chick, J.; Inuzuka, H.; Li, X.; Mansour, M. R.; Liu, L.; Wang, H.; King, B.; Shaik, S.; Gutierrez, A.; Ordureau, A.; Otto, T.; Kreslavsky, T.; Baitsch, L.; Bury, L.; Meyer, C. A.; Ke, N,; Mulry, K. A.; Kluk, M. J.; Roy, M.; Kim, S.; Zhang, X.; Geng, Y.; Zagozdzon, A.; Jenkinson, S.; Gale, R. E.; Linch, D. C.; Zhao, J. J.; Mullighan, C. G.; Harper, J. W.; Aster, J. C.; Aifantis, I.; von Boehmer, H.; Gygi, S. P.; Wei, W.; Look, A. T.; Sicinski, P. *Nat. Cell Biol.* **2014**, *16*, 1080–1091.

15. Alacón, C.; Zaromytidou, A. I.; Xi, Q.; Gao, S.; Yu, J.; Fujisawa, S.; Barlas, A.; Miller, A. N.; Manova-Todorova, K.; Macias, M. J.; Sapkota, G.; Pan, D.; Massaqué, J. *Cell* **2009**, *139*, 757–769.

16. Xu, D.; Li, C.-F.; Zhang, X.; Gong, Z.; Chan, C.-H.; Lee, S.-W.; Jin, G.; Rezaeian, A.-H.; Han, F.; Wang, J.; Yang, W.-L.; Feng, Z.-Z.; Chen, W.; Wu, C.-Y.; Wang, Y.-J.; Chow, L.-P.; Zhu, X.-F.; Zeng, Y.-X.; Lin, H.-K. *Nat. Commun.* **2015**, *6*, 6641.

17. (a) Adler, A. S.; McCleland, M. L.; Truong, T.; Lau, S.; Modrusan, Z.; Soukup, T. M.; Roose-Girma, M.; Blackwood, E. M.; Firestein, R. *Cancer Res.* **2012**, *72*, 2129–2139; (b) McCleland, M. L.; Soukup, T. M.; Liu, S. D.; Esensten, J. H.; de Sousa e Melo, F.; Yaylaoglu, M.; Warming, S.; Roose-Girma, M.; Firestein, R. *J. Pathol.* **2015**, *237*, 508–519.

18. Brägelmann, J.; Klümper, N.; Offermann, A.; von Mässenhausen, A.; Böhm, D.; Deng, M.; Queisser, A.; Sanders, C.; Syring, I.; Merseburger, A. S.; Vogel, W.; Sievers, E.; Vlasic, I.; Carlsson, J.; Andrén, O.; Brossart, P.; Duensing, S.; Svensson, M. A.; Shaikhibrahim, Z.; Kirfel, J.; Perner, S. *Clin. Cancer. Res.* **2016**, ASAP.

19. (a) Roninson, I. World Patent 2013040153, March, 21, 2013; (b) Robinson, I. B.; Porter, D. C.; Wentland, M. P. World Patent 2013116786, August, 8, 2013. (c) Roninson, I.; Chen, M. World Patent

2014071143, May, 8, 2014; (d) Broude, E.; Roninson, I. B. World Patent 2014134169, September, 4, 2014; (e) Roninson, I. B.; Cui, T. World Patent 2016100782, June, 23, 2016.

20. Pastor Fernández, J.; Álvarez Escobar, R. M.; Varela Busto, C.; García García, A. B.; Dimitrievich Zarich, N.; Blanco Aparicio, C.; Rodríguez López, A.; Oyarzabal Santamarina, J.; Bischoff, J. R. World Patent 2013001310, January, 3, 2013.

21. Rzymski, T.; Zarebski, A.; Dreas, A.; Osowska, K.; Kucwaj, K.; Fogt, J.; Cholody, M.; Galezowski, M.; Czardybon, W.; Horvath, R.; Wiklik, K.; Milik, M.; Brzózka, K. World Patent 20141072435, May, 15, 2014.

22. Cheng, Z.; Han, X.; Jiang, M.; Wang, J.; Wang, M.; Yang, S.; Zhou, C. World Patent 20141090692, June, 19, 2014.

23. (a) Hu, H.; Jiang, M.; Jin, T.; Niu, R.; Wang, J.; Yang, S.; Yuan, T.; Zhou, C.; Wang, M.; Zhou, Z. World Patent 20141029726, February, 27, 2014; (b) Wang, J.; Wang, M.; Yang, S.; Zhou, C. World Patent 2014106606, July, 10, 2014.

24. Han, X.; Jiang, M.; Mayweg, A. V.; Wang, L.; Yang, S. World Patent 2014154723, October, 2, 2014.

25. Romero, D. L.; Chaudhary, D.; Robinson, S.; Masse, C. E.; Morin, M. J. World Patent 2014194201, December, 4, 2014.

26. (a) Pelish, H. E.; Liau, B. B.; Nitulescu, I. I.; Tangpeerachaikul, A.; Poss, Z. C.; Da Silva, D. H.; Caruso, B. T.; Arefolov, A.; Fadeyi, O.; Christie, A. L.; Du, K.; Banka, D.; Schneider, E. V.; Jestel, A.; Zou, G.; Si, C.; Ebmeier, C. C.; Bronson R. T.; Krivtsov, A. V.; Myers, A. G.; Kohl, N. E.; Kung, A. L.; Armstrong, S. A.; Lemieux, M. E.; Taatjes, D. J.; Shair, M. D. *Nature* **2015**, *526*, 273–276; (b) Dale, T.; Clarke, P. A.; Esdar, C.; Waalboer, D.; Adeniji-Popoola, O.; Ortiz-Ruiz, M.-J.; Mallinger, A.; Samant, R. S.; Czodrowski, P.; Musil, D.; Schwarz, D.; Schneider, K.; Stubbs, M.; Ewan, K.; Fraser, E.; TePoele, R.; Court, W.; Box, G.; Valenti, M.; de Haven Brandon, A.; Gowan, S.; Rohdich, F.; Raynaud, F.; Schneider, R.; Poeschke, O.; Blaukat, A.; Workman, P.; Schiemann, K.; Eccles, S. A.; Wienke, D.; Blagg, J. *Nat. Chem. Biol.* **2015**, *11*, 973–980; (c) Boyer, T. G. *Nat. Chem. Biol.* **2016**, *12*, 4–5.

27. (a) Aoki, S.; Watanabe, Y.; Sanagawa, M.; Setiawan, A.; Kotoku, N.; Kobayashi, M. *J. Am. Chem. Soc.* **2006**, *128*, 3148–3149; (b) Cee, V. J.; Chen, D. Y.-K.; Lee, M. R.; Nicolaou, K. C. *Angew. Chem. Int. Ed.* **2009**, *48*, 8952–8957.

28. Poss, Z. C.; Ebmeier, C. C.; Odell, A. T.; Tangpeerachaikul, A.; Lee, T.; Pelish, H. E.; Shair, M. D.; Dowell, R. D.; Old, W. M.; Taatjes, D. J. *Cell Rep.* **2016**, *15*, 436–450.

29. (a) Schiemann, K.; Stieber, F.; Blagg, J.; Mallinger, A.; Waalboer, D.; Rink, C.; Crumpler, S. R. World Patent 2014063778, May, 1, 2014; (b) Mallinger, A.; Crumpler, S.; Pichowicz, M.; Waalboer, D.; Stubbs, M.; Adeniji-Popoola, O.; Wood, B.; Smith, E.; Thai, C.; Henley, A. T.; Georgi, K.; Court, W.; Hobbs, S.; Box, G.; Ortiz-Ruiz, M.-J.; Valenti, M.; de Haven Brandon, A.; TePoele, R.; Leuthner, B.; Workman, P.; Aherne, W.; Poeschke, O.; Dale, T.; Wienke, D.; Esdar, C.; Rohdich, F.; Raynaud, F.; Clarke, P. A.; Eccles, S. A.; Stieber, F.; Schiemann, K.; Blagg, J. *J. Med. Chem.* **2015**, *58*, 1717–1735.

30. Mallinger, A.; Schiemann, K.; Rink, C.; Stieber, F.; Calderini, M.; Crumpler, S.; Stubbs, M.; Adeniji-Popoola, O.; Poeschke, O.; Busch, M.; Czodrowski, P.; Musil, D.; Schwarz, D.; Ortiz-Ruiz, M.-J.;

Schneider, R.; Thai, C.; Valenti, M.; de Haven Brandon, A.; Burke, R.; Workman, P.; Dale, T.; Wienke, D.; Clarke, P. A.; Esdar, C.; Raynaud, F. I.; Eccles, S. A.; Rohdich, F.; Blagg, J. *J. Med. Chem.* **2016**, *59*, 1078–1101.

31. (a) Schiemann, K.; Blagg, J.; Mallinger, A.; Rink, C.; Sejberg, J.; Honey, M. World Patent 2016009076, January, 21, 2016; (b) Mallinger, A.; Schiemann, K.; Rink, C.; Sejberg, J.; Honey, M. A.; Czodrowski, P.; Stubbs, M.; Poeschke, O.; Busch, M.; Schneider, R.; Schwarz, D.; Musil, D.; Burke, R.; Urbahns, K.; Workman, P.; Wienke, D.; Clarke, P. A.; Raynaud, F. I.; Eccles, S. A.; Esdar, C.; Rohdich, F.; Blagg, J. *ACS Med. Chem. Lett.* **2016**, *7*, 573–578.

32. (a) Schiemann, K. World Patent 2016041618, March, 24, 2016; (b) Schiemann, K.; Mallinger, A.; Wienke, D.; Esdar, C.; Poeschke, O.; Busch, M.; Rohdich, F.; Eccles, S. A.; Schneider, R.; Raynaud, F. I.; Czodrowski, P.; Musil, D.; Schwarz, D.; Urbahns, K.; Blagg, J. *Bioorg. Med. Chem. Lett.* **2016**, *26*, 1443–1451.

33. (a) Schiemann, K.; Mallinger, A. Indazoles. World Patent 2016026549, February, 25, 2016; (b) Czodrowski, P.; Mallinger, A.; Wienke, D.; Esdar, C.; Poschke, O.; Busch, M.; Rohdich, F.; Eccles, S. A.; Ortiz-Ruiz, M.-J.; Schneider, R.; Raynaud, F. I.; Clarke, P. A.; Musil, D.; Schwarz, D.; Dale, T. C.; Urbahns, K.; Blagg, J.; Schiemann, K. *J. Med. Chem.* **2016**, *59*, ASAP.

34. Koehler, M. F.; Bergeron, P.; Blackwood, E. M.; Bowman, K.; Clark, K. R.; Firestein, R.; Kiefer, J. R.; Maskos, K.; McCleland, M. L.; Orren, L.; Salphati, L.; Schmidt, S.; Schneider, E. V.; Wu, J.; Beresini, M. H. *ACS Med. Chem. Lett.* **2016**, *7*, 223–228.

35. (a) Bergeron, P.; Koehler, M. World Patent 2015049325, April, 9, 2015; (b) Bergeron, P.; Koehler, M. F. T.; Blackwood, E. M.; Bowman, K.; Clark, K.; Firestein, R.; Kiefer, J. R.; Maskos, K.; McCleland, M. L.; Orren, L.; Ramaswamy, S.; Salphati, L.; Schmidt, S.; Schneider, E. V.; Wu, J.; Beresini, M. *ACS Med. Chem. Lett.* **2016**, *7*, 595–600.

36. (a) Yasuma, T.; Oda, T.; Hazama, M.; Taketomi, S. World Patent 199809958, March, 2, 1998; (b) Yasuma, T.; Mori. A.; Kawase, M.; Takizawa, M.; Miki, S.; Takeda, M. World Patent 2001074823, October, 11, 2001; (c) Oka, M.; Yamada, Y. World Patent 2012036293, March, 22, 2012.

37. Motoyaji, T. *et al.* Manuscript in preparation.

38. Schneidera, E. V.; Bottcherb, J.; Hubera, R.; Maskosb, K.; Neumannb, L. *Proc. Natl. Acad. Sci. USA*, **2013**, *110*, 8081–8086.

39. For related work by our group, see also: (a) Okaniwa, M.; Banno, H.; Hirayama, T.; Cary, D. R.; Ono, K.; Iwamura, N. World Patent 2015159937, October, 22, 2015; (b) Hirayama, T.; Fujimoto, J.; Cary, D. R.; Okaniwa, M.; Hirata, Y. World Patent 2015159938, October, 22, 2015; (c) Fujimoto, J.; Hirayama, T.; Hirata, Y.; Hikichi, Y.; Murai, S.; Hasegawa, M.; Hasegawa, Y.; Yonemori, K.; Hata, A.; Aoyama, K.; Cary, D. R. *Bioorg. Med. Chem.*, submitted for publication.

40. For a representative review, see: Roy, S.; Roy, S. Gribble, G. W. *Tetrahedron* **2012**, *68*, 9867–9923.

41. (a) Lagerlund, O.; Larhed, M. *J. Comb. Chem.* **2006**, *8*, 4–6; (b) Iizuka, M.; Kondo, Y. *Chem. Commun.* **2006**, 1739–1741; (c) Begouin, A.; Queiroz, M.-J. R. P. *Eur. J. Org. Chem.* **2009**, 2820–2827; (d) Lagerlund, O.; Mantel, M. L. H.; Larhed, M. *Tetrahedron* **2009**, *65*, 7646–7652; (e) Nordeman, P.; Odell, L.

R.; Larhed, M. *J. Org. Chem.* **2012**, *77*, 11393–11398.

42. For selected reviews, see: (a) Barnaed, C. F. J. *Organometallics*, **2008**, *27*, 5402–5422; (b) Brennführer, A.; Neumann, H.; Beller, M. *Angew. Chem. Int. Ed.* **2009**, *48*, 4114–4133 (c) Wu, X.-F.; Neumann, H.; Beller, M. *Chem. Soc. Rev.* **2011**, *40*, 4986–5009; (d) Wu, X.-F.; Neumann, H.; Beller, M. *Chem. Rev.* **2013**, *113*, 1–35.

43. For a recent review: Metal-catalyzed cross-coupling reactions and more; de Meijere, A.; Bräse, S.; Oestreich, M. Eds.; Wiley-VCH: Weinheim, 2014; pp 995–1066.

44. For selected reviews, see: (a) Buchwald, S. L.; Mauger, C.; Mignani, G.; Scholz, U. *Adv. Synth. Catal.* **2006**, *348*, 23–39; (b) Surry, D. S.; Buchwald, S. L. *Angew. Chem. Int. Ed.* **2008**, *47*, 6338–6361; (c) Hartwig, J. F. *Acc. Chem. Res.* **2008**, *41*, 1534–1544; (d) Torborg, C.; Beller, M. *Adv. Synth. Catal.* **2009**, *351*, 3027–3043; (e) Surry, D. S.; Buchwald, S. L. *Chem. Sci.* **2011**, *2*, 27–50.

45. For a selected review, see: (a) Zhong, H. A.; Mashinson, V.; Woolman, T. A. Zha, M. *Curr. Top. Med. Chem.* **2013**, *13*, 1290–1307.

46. Fabian, M. A.; Biggs, W. H. 3rd.; Treiber, D. K.; Atteridge, C. E.; Azimioara, M. D.; Benedetti, M. G.; Carter, T. A.; Ciceri, P.; Edeen, P.T.; Floyd, M.; Ford, J. M.; Galvin, M.; Gerlach, J. L.; Grotzfeld, R. M.; Herrgard, S.; Insko, D. E.; Insko, M. A.; Lai, A. G.; Lélias, J. M.; Mehta, S. A.; Milanov, Z. V.; Velasco, A. M.; Wodicka, L. M.; Patel, H. K.; Zarrinkar, P. P.; Lockhart, D. J. *Nat. Biotechnol.* **2005**, *23*, 329−336.